Jet structure in e^+e^- annihilation as a test of quantum chromodynamics and the quark-confining string*

T. A. DeGrand, Yee Jack Ng, and S.-H. H. Tye
Stanford Linear Accelerator Center, Stanford University, Stanford, California 94305
(Received 20 June 1977)

We examine the jet structure in e^+e^- annihilation from two processes: (a) the bremsstrahlung of a hard gluon and (b) the emission of a meson at wide angle via the constituent-interchange model (CIM). At center-of-mass energies from 12 to 25 GeV, both processes, if present, are found to broaden the sharp transverse-momentum damping of jets observed at SPEAR. At lower energies and large transverse momentum we find that the CIM process prevails. But by center-of-mass energies greater than 30 GeV the gluonic process should be dominant. We also examine the jet structure generated by the decay of a bound state of new heavy quarks into three gluons. Should such quarks ($m_q \gtrsim 5$ GeV) exist, this bound state would provide an ideal place to look for gluon-induced jets. Other topics we have studied include (i) jet structure via the production of four quarks and (ii) different possible gluonic fragmentation functions. Jet structure in deep-inelastic lepton-hadron scattering processes is also briefly considered. We conclude that e^+e^- annihilation is probably the cleanest place to search for gluonic structure, whose existence would be striking evidence in favor of quantum chromodynamics (QCD). On the other hand, the absence of such structure would necessitate a reexamination of our intuitive understanding of QCD and a serious consideration of other field-theoretical hadronic models, e.g., the quark-confining string, which, unlike QCD, does not possess gluonic degrees of freedom.

I. INTRODUCTION

One of the most striking discoveries which has emerged from the study of electron-positron annihilation at SPEAR[1] is the observation that at center-of-mass energies greater than 5 GeV, hadrons are produced predominantly in back-to-back bursts, called jets. These jets are characterized by three distinct signals: first, the transverse momentum of hadrons in the jet relative to the jet axis is sharply cut off on a scale of a few hundred MeV. Second, the distribution of hadrons in the jet longitudinal to the jet axis is a function only of the fraction of the jet momentum carried by the hadrons, and depends only weakly on the absolute center-of-mass energy of the electron-positron system; and finally, the distribution of jets relative to the axis of the incoming electron and positron momentum is, to good accuracy, $1+\cos^2\theta$, where θ is the angle between the jet and that axis.

These observations are most simply explained by the parton picture[2] of hadron substructure: e^+e^- annihilation into hadrons proceeds via e^+e^- annihilation into a quark-antiquark pair. At short distances, the quarks behave as if they were free; the $1+\cos^2\theta$ angular distribution which is observed is characteristic of e^+e^- annihilation into a pair of spinors. At long distances, quarks are confined and hence must fragment into hadrons. This conclusion is bolstered by the earlier observation that the ratio of cross sections $\sigma(e^+e^-\to\text{hadrons})/\sigma(e^+e^-\to\mu^+\mu^-)$ is roughly a constant which changes only when the threshold for producing new quantum numbers (or hadrons containing new flavors of quarks) is crossed.

In recent years, the parton model has found an elegant realization in quantum chromodynamics (QCD),[3] the local, asymptotically free field-theoretic model of triplet quarks interacting with colored vector gluons.[4] QCD provides a natural explanation for Bjorken scaling in deep-inelastic lepton-hadron scattering and (to a lesser extent) the jet structure in e^+e^- annihilation. However, it is an open question whether or not quarks are confined in QCD. To determine whether QCD actually exhibits quark confinement and, furthermore, whether it gives a spectrum of hadrons with their observed properties, is a very formidable task.[5] Since more theoretical efforts will certainly be directed towards this issue, it is important to examine all available experimental evidence that may support QCD.

It is clear that many experimental facts can be explained naturally by QCD. The question we want to address ourselves to is whether there is any experimental evidence that supports QCD unambiguously. To formulate this question more concretely and explicitly, we must compare QCD to some other hadronic models. Noticing that QCD possesses, in addition to the quarks, gluonic degrees of freedom, it is natural to compare it to a specific hadronic model which does not have gluonic degrees of freedom. In particular, we have in mind the quark-confining string (QCS) model.[6]

The quark-confining string is defined by a relativistic-invariant, gauge-invariant, and reparam-

etrization-invariant action of color quarks interacting with color SU(3) Yang-Mills fields along a string. It is a field-theoretic model where quarks are Dirac fields in Minkowski space while the gauge fields have no independent degrees of freedom. The physical picture of QCS closely resembles that expected from QCD. In fact, in two-dimensional Minkowski space, the two models are identical. Quark confinement is explicit in the QCS. (See Appendix A for a brief summary of the properties of the QCS that are relevant to this work.)

The key qualitative difference between QCD and the QCS is the absence of gluonic degrees of freedom in the latter. One may consider the QCS as a phenomenological model of QCD, so that it can be used to study the sector of hadron physics where gluonic degrees of freedom do not play any major role but where confinement effects are important. Since it is very difficult to calculate nonperturbative properties of QCD, the QCS provides a very handy tool for calculating various hadronic properties such as spectroscopy. For the sake of comparison, we shall take the QCS to be a phenomenological but complete working model in its own right (see Fig. 1).

Since QCD possesses gluonic degrees of freedom[7] and the QCS does not, a comparison of these models with experiments will sharpen effects of the existence or absence of gluonic structure. At present, the existence of gluons is often inferred from two experimental observations.

The first is Bjorken scaling. Since QCD is asymptotically free, the proton's constituents admit to a parton interpretation in the deep-inelastic region. In the QCS, one also expects a parton picture to emerge; the quark-quark potential is linear, hence vanishing at short distances. The question of corrections to scaling is more difficult. Scaling seems not to be exact at the highest Q^2, ν yet measured; both QCD and the QCS may be consistent with scaling violations. In the former case these violations arise from pieces of various gluon-exchange graphs, calculated via the renormalization group.[8] In the latter case it is possible that scaling is broken by the quantum fluctuations of the string. Since the string is quite rigid (vibrational energies are greater than radial or rotational energies[9]), these corrections to scaling in the QCS are probably small. We must point out that, while the explanation of scale breaking via asymptotic freedom is attractive, it is by no means proven.[10]

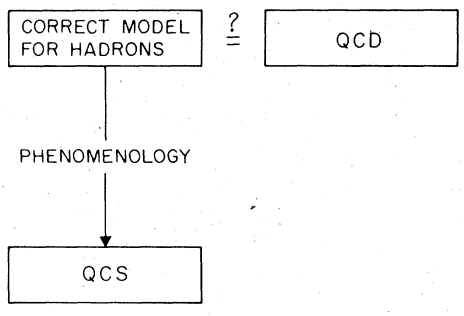

FIG. 1. Schematic form of the relation between quantum chromodynamics (QCD), the quark-confining string (QCS) model, and the correct model of hadrons.

The second observation which is occasionally cited to infer the existence of gluons is that the momentum sum rule of e^-p scattering is not saturated by charged constituents; about half of the momentum of the proton is carried by neutral partons. In QCD, these neutral partons are presumed to be the colored gluons. The QCS picture is equally simple; in the (nonrelativistic) application of the QCS to the ψ spectroscopy[9] we learn that for the $\psi(3.1)$, the potential energy (i.e., the string energy) is, using the virial theorem, roughly,

$$\tfrac{2}{3}(M-2m)\sim 0.5\ \text{GeV}.$$

$M(\sim 3.1\ \text{GeV})$ is the mass of the state ψ and $m(\sim 1.15\ \text{GeV})$ is the mass of the charmed quark. As $m\to 0$, the fraction of energy-momentum carried by the (neutral part of the) string increases. An order-of-magnitude estimate of the fraction of energy carried by the string can be obtained by the following consideration. For a ground-state light hadron ($m\sim 0$)

$$E(R)=\frac{f(n,R)}{R}+kR=E_f+E_s,$$

where the first term is the quark kinetic (fermionic) energy and the second term is the string energy. n is the number of quarks (antiquarks) present in the hadron. f and k are, at most, slowly varying functions of R, the length of the physical string; they are taken to be constants in this simple approximation. Minimizing $E(R)$, $\partial E(R)/\partial R=0$ gives

$$E(R_0)\sim 2\sqrt{fk},$$

$$E_f\sim E_s\sim E/2.$$

Therefore we expect the charged quarks to carry roughly half the hadron's energy-momentum. Since the string energy arises from a vector potential, this remains true in any Lorentz frame. Hence the momentum sum rule in deep-inelastic scattering can be satisfied without invoking the existence of gluons. This allows us to conclude that, at the present moment, there is no unambiguous experimental evidence for the existence

of colored gluonic degrees of freedom.[11]

Since these two tests of the existence of gluons are inconclusive, what are the other alternatives? One possibility would be the observation of hadrons which do not contain quarks, only gluons, i.e., quarkless states. This test would be most difficult to verify. To begin with, we do not know if such states are allowed in QCD (although they are predicted by lattice gauge theories[5] or by the MIT bag model[7] to have masses starting at 1-2 GeV[12]). These states are flavor SU(4) singlets, hence hard to observe. A typical characteristic is their small leptonic width (for 1^- states). However, they probably mix with ordinary quark-antiquark states with the same quantum numbers, and then can interact like ordinary mesons, through the quark part of their wave functions. This renders the identification of quarkless states difficult. In the QCS, vibrational levels (with spin-parity assignment 1^-) are expected to have very small leptonic widths also. For light mesons, the lowest vibrational states also have masses starting around 1-2 GeV. Hence it will be difficult to tell a quarkless state from a vibrational state of a flavorless meson and a search for quarkless states may not be the best place to look for the existence of gluons.

The best test for the existence of gluons we know is via scattering experiments which probe small hadronic distances. If gluons exist, they must be produced in such reactions just as quarks are, and then fragment into color singlet hadrons much as quarks do. Jets which are presumed to arise from quark scattering and fragmentation, are seen in wide-angle pp inclusive scattering, deep-inelastic scattering, and in the production of hadrons in e^+e^- annihilation.[13] Hard-gluon production should manifest itself as a broadening of the transverse-momentum distribution of these jets, and also in the formation of extra jets in these reactions at higher energies.[14-16] In this work we examine in detail the structure of the jets produced in e^+e^- annihilation.

Since precise quantitative calculations of jet structures starting from QCD or the QCS are not possible at the present moment, we shall abstract a phenomenology from them so that they satisfy the present experimental situation. In particular we assume QCD has quark confinement at present energies and that the fragmentation of quarks into hadrons leads to the jet structure observed at SPEAR and elsewhere. In the e^+e^- channel, both QCD and the QCS are taken to explain the jet structure at higher SPEAR energies via the following picture of the parton model:

(1) e^+e^- annihilate to a virtual photon which then decays into a quark-antiquark pair ($q\bar{q}$). The latter are essentially free when they are created [see Fig. 2(a)].

(2) As the $q\bar{q}$ move away from each other, they fragment into hadrons with little transverse momenta. The resulting momentum distribution of the hadrons has a cigar shape with a transverse-momentum cutoff around 0.35 GeV. This is illustrated in Fig. 2(b).

We now wish to consider an extension of this basic process. In QCD, before the quarks fragment into (color singlet) hadrons, the quarks can interact via the following two processes: (a) bremsstrahlung of a colored vector gluon, and (b) emission of a hadron (typically a pion) at wide angle.

The QCS has no gluons, hence the gluon bremsstrahlung process is absent. It seems plausible that emission of a pion at wide angle will take place in the QCS. Intuitively, the QCS is expected to have both an exponential transverse-momentum distribution from the string modes and a powerlike contribution from the quark modes. This conjecture is not unreasonable since the QCS can be considered as a synthesis of the dual string[17] and two-dimensional QCD.[18] It is our hope that, since the existence or absence of the gluon structure is such a gross feature, and that, if present, the signal is so distinct, that the jet structure test should be relatively insensitive to the detailed assumptions we make for QCD and the QCS.

The broadening of the jet structure due to gluon bremsstrahlung has been studied in detail by

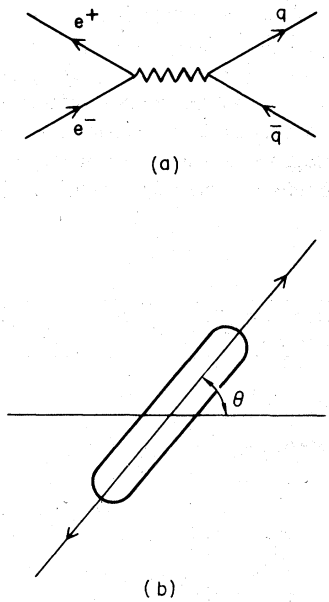

FIG. 2. (a) Lowest-order process for $e^+e^- \to$ hadrons and (b) its two-jet structure in momentum space.

Ellis, Gaillard, and Ross (EGR).[16] The calculation proceeds via three steps:

(1) First, the initial gluon-quark interaction is calculated from Feynman diagrams. This is justified by asymptotic freedom.

(2) Next, this approach is carried one step further; as long as all invariant subenergies of the final-state quarks and gluons are large, the color coupling constant α_c is small enough that perturbation theory is applicable; gluon emission is calculated perturbatively in α_c.

(3) Finally, the quarks and gluons fragment into color singlet hadrons. The fragmentation function is extracted from the SPEAR data. In principle, this metamorphosis of the quark or gluon into hadrons is due to quark confinement. In practice, one merely folds the fragmentation functions over the final-state quarks and gluons.

To calculate the emission of a pion from a quark, we apply the constituent-interchange model (CIM) and dimensional counting (DC).[19] Since CIM and DC describe hadronic scattering quite successfully, we shall assume in this work that both QCD and the QCS have these properties. Hence the presence or absence of a wide-angle pion emission process does not test either QCD or the QCS. An understanding of this process allows us to separate it from gluon bremsstrahlung events, if the latter exists. Incidentally, if this pion emission process contributes to the broadening of jet structure, as one expects, e^+e^- annihilation into hadrons is probably the cleanest place to determine the normalization of the quark-meson coupling of the CIM.

We find that at c.m. energies in the range 12–25 GeV both gluon bremsstrahlung and CIM pion emission broaden the sharp transverse-momentum damping of jets observed at SPEAR. At lower energies, the CIM process dominates. However, due to the different Q^2 (Q is the center-of-mass energy of the e^+e^- system) behavior of the gluon and CIM processes [differential cross sections $(1/\sigma_{\text{tot}})d\sigma/dQ^2 \propto Q^{-2}$ and Q^{-4}, respectively], gluon bremstrahlung, if present, eventually becomes the most important source of jet broadening; with a reasonable value of α_c and with normalization for the CIM process taken from the scattering experiments or extracted (as an upper limit) from SPEAR data, the gluonic process should be dominant at c.m. energies greater than 30 GeV. It would be important to push PEP and PETRA to even higher energies in order that this effect be as striking as possible.

We have also considered modifications of the gluon-bremsstrahlung picture in two ways. First, we have investigated the behavior of the cross section with respect to different gluon fragmentation functions; we find that our results are not too sensitive to the form of the fragmentation function. Second, we have considered the possibility that the gluon might break into a $q\bar{q}$ pair before fragmenting into hadrons. This process leads to another scale-invariant contribution to the cross section which could be a fair fraction of the single-gluon bremsstrahlung cross section.

Another place where gluon jets may be visible would be in the decay of a bound state of heavy quarks carrying new quantum numbers. The decays of this state would be Zweig-forbidden and would proceed via an intermediate state of three gluons. If the mass of the state is large enough, the gluons may form jets as they decay into ordinary hadrons. We have calculated the inclusive momentum distribution of hadrons which would be expected from the fragmentation of the three gluons, and find that, if gluons exist, their presence should be easily discernible in the decays of the new state. Of course, this three-jet dominance is completely absent in the QCS.

Finally, we have investigated the related problem of jets and their broadening in deep-inelastic electroproduction. We have used the "eikonal" approximation to estimate the relative importance of gluon emission and the CIM process. We find that the CIM is the dominant contributor to jet broadening in currently accessible regions of energy and momentum transfer.

We outline this paper as follows. Section II contains a study of gluonic bremsstrahlung. This section is mainly a review and an extension of the earlier work of Ellis, Gaillard, and Ross. The other major contribution to the broadening of the jet structure is discussed in Sec. III, i.e., hard-scattering processes which are the analogs of meson-quark scattering in the constituent-interchange model. In Sec. IV we consider the jet structure generated by the production of four quarks in e^+e^- annihilation. Section V deals with the jet structure expected from the decay of a bound state of new heavy quarks (should they exist). This will be a good laboratory in which to look for the effects of gluons; should gluons exist, the spin-one state will decay via three gluons, producing a striking three-jet pattern. In Sec. VI we briefly consider the broadening of the transverse-momentum distribution in the inclusive deep-inelastic lepton-hadron scattering due to both the CIM process and the existence of gluons. This is compared to the broadening of jet structure in e^+e^- annihilation. Section VII contains our conclusions. There are two appendices. Appendix A summarizes the features of the QCS that are relevant to this work. Appendix B contains the various details of the four-quark jet calculations.

II. GLUON BREMSSTRAHLUNG

In this section we review and set up the notation for the gluon bremsstrahlung process $e^+e^- \to \gamma \to q\bar{q}G$ (Fig. 3), where q and $\bar{q}$ are the colored quark and antiquark, and G is a colored vector gluon. To obtain the cross sections for e^+e^- annihilation in QCD, a number of simplifying assumptions shall be made. Some of these assumptions will be examined later. For the case in which q, $\bar{q}$, and G each carries a sizable fraction of the total energy, the resulting event looks like three jets instead of two jets. For the QCS, there is no such three-jet producing mechanism and hence the two-jet structure persists for all e^+e^- energies. This is the preliminary result. In Sec. III we examine the broadening of the two-jet structure due to the emission of a meson.

The gluon bremsstrahlung process has been calculated by EGR.[16] The calculation proceeds as follows: (1) the quark and the gluon produced in $e^+e^- \to q\bar{q}G$ are folded into their respective fragmentation functions, each having a sharp transverse-momentum cutoff; (2) the jet axis is found by minimizing the total transverse momenta of all hadrons; and (3) the broadening of the jet axis is given in terms of distributions in $x_\perp = 2p_\perp/Q$, where $p_\perp$ is the transverse momentum of a hadron with respect to the jet axis and Q is the total energy in the center-of-mass frame. The e^+, e^-, q, $\bar{q}$, and G momenta are defined in Fig. 3. They have energies E, E, E_1, E_2, and E_3, respectively. The three final-state particles lie in a plane whose normal makes an angle θ to the e^+ momentum $\vec{q}_1$. The virtual photon has energy $Q = 2E$ in its rest frame. Since all energies to be considered are large, it is reasonable to neglect all masses. The Feynman diagrams of Fig. 3 give a cross section

$$d\sigma = \frac{1}{2(2\pi)^5}\delta^4(q_1+q_2-p_1-p_2-p_3)|M|^2 \times \frac{d^3p_1}{2E_1}\frac{d^3p_2}{2E_2}\frac{d^3p_3}{2E_3}\frac{1}{(2E)^2}, \tag{2.1}$$

where M is the matrix element. Averaging the initial polarizations and summing over the final-state polarizations give

$$|M|^2 = \frac{e^4g^2}{4Q^4} L^{\mu\nu}H_{\mu\nu}, \tag{2.2}$$

where the lepton trace is

$$L^{\mu\nu} = \mathrm{Tr}\gamma^\mu \not{q}_1 \gamma^\nu \not{q}_2 \equiv 4\{q_1, q_2\}^{\mu\nu}, \tag{2.3}$$

and the hadron trace is

$$\tfrac{1}{4}H_{\mu\nu} = \frac{1}{p_1\cdot p_3}[\{p_2,p_3\}_{\mu\nu}+\{p_1,p_2\}_{\mu\nu}-\{p_1,p_1\}_{\mu\nu}] + \frac{1}{p_2\cdot p_3}[\{p_1,p_3\}_{\mu\nu}+\{p_1,p_2\}_{\mu\nu}-\{p_2,p_2\}_{\mu\nu}] + \frac{p_1\cdot p_2}{(p_1\cdot p_3)(p_2\cdot p_3)}[2\{p_1,p_2\}_{\mu\nu}+\{p_1,p_3\}_{\mu\nu} + \{p_2,p_3\}_{\mu\nu}]. \tag{2.4}$$

Introducing the variables

$$s_{ij} = (p_i+p_j)^2 = 2p_i\cdot p_j = Q^2(1-x_k) \tag{2.5}$$

for $i \neq j \neq k$, where $x_i = E_i/E = 2E_i/Q$, the cross section can be written as

$$d\sigma = \frac{1}{(2\pi)^5}\frac{1}{32Q^2}ds_{13}ds_{23}d\cos\theta\, d\chi\, d\phi\, \frac{|M|^2}{2Q^2}, \tag{2.6}$$

where χ is the orientation angle of the plane and ϕ is the azimuthal angle. Integrating over these two angles, we arrive at the differential cross section

$$\frac{d\sigma}{dx_1dx_2} = \left(\sum_a q_a^2\right)\frac{\alpha^2\alpha_c}{8Q^2}\frac{x_1^2+x_2^2}{(1-x_1)(1-x_2)} \times (2+\sin^2\theta)\,d(\cos\theta) \tag{2.7}$$

(notice that EGR have erred in their definition of θ), where $\alpha_c = g_c^2/4\pi$ is the quark-gluon structure constant, and q_a is the fraction of unit electric charge of the quark with flavor index a. α is the QED fine-structure constant. Assuming scaling and color SU(3), we write the pointlike cross section

$$\sigma_{pt}(e^+e^- \to \gamma \to X) = 3\sum_a q_a^2\sigma(e^+e^- \to \gamma \to \mu^+\mu^-) = \frac{4\pi}{Q^2}\alpha^2\sum q_a^2. \tag{2.8}$$

Integrating the angles in Eq. (2.7) and including a factor of 4 coming from color summation, we obtain the normalized cross section

$$\frac{1}{\sigma_{pt}}\frac{d\sigma}{dx_1dx_2} = \frac{2}{3}\frac{\alpha_c}{\pi}\frac{x_1^2+x_2^2}{(1-x_1)(1-x_2)}. \tag{2.9}$$

To extract meaningful, physically observable quantities from the above Feynman graph calculation, we must ensure that we always remain in

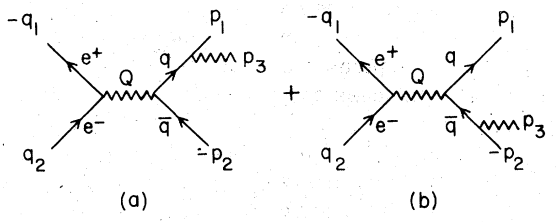

FIG. 3. Feynman graphs for $e^+e^- \to q\bar{q}G$, with the labeling of momenta used in the text.

the kinematic domain where perturbation calculations are valid. In the e^+e^- channel, scaling sets in quite early for the light quarks. In the language of QCD, this means the effective quark-gluon color coupling is small enough at the approximate scaling region so that perturbation calculations are reliable. Following EGR, we take that value to be $Q_0^2 \sim 10$ GeV^2 and study the kinematic regions where the invariants s_{13}, s_{23}, and s_{12} are all bigger than Q_0^2. For small s_{ij}, the transverse momentum of any one jet with respect to the jet axis becomes small. Hence this cutoff (in Q_0^2) has little effect on the large transverse-momentum part of the differential cross section. In the x variables, we have

$$Q_0^2/Q^2 \equiv \epsilon, \qquad 2\epsilon < x_i < 1-\epsilon, \quad i=1,2,3. \tag{2.10}$$

Thus the total three-jet cross section $\sigma_{3\,\mathrm{jet}}$ is

$$\frac{1}{\sigma_{\mathrm{pt}}}\sigma_{3\,\mathrm{jet}} = \frac{2}{3}\frac{\alpha_c}{\pi}\int_{2\epsilon}^{1-\epsilon} dx_1 \int_{2\epsilon} dx_2 \frac{x_1^2+x_2^2}{(1-x_1)(1-x_2)} \sim \frac{4}{3}\frac{\alpha_c}{\pi}|\ln\epsilon|^2. \tag{2.11}$$

Second, we must connect our Feynman graphs involving quarks and gluons to the real world of hadrons. We do this in the standard manner by describing the fragmentation of quarks and gluons into hadrons by a fragmentation function $f(x)$, where x is the fraction of longitudinal momentum carried off by the hadron. The following quark fragmentation function, which provides a good fit to SPEAR data,[1] has been given by EGR:

$$xf(x) = 2.2(1-x)^3 + 0.25(1-x). \tag{2.12}$$

Since neutral hadrons are not observed, $\int xf(x)\,dx$ is normalized to $\frac{2}{3}$ rather than 1.

What should the gluon fragmentation function be? This is a problem, as gluon fragmentation has not been observed. We may take several alternatives. First, the gluon function $g(x)$ may be taken to be equal to the quark function. Second, we may take

$$g(x) = 1.23(1-x)f(x). \tag{2.13a}$$

The latter form is motivated by the theoretical prejudices that $g(x)$ should peak more at lower x than $f(x)$ (such a form is suggested by constituent-interchange models[20]) and that $g(x)$ should have the same normalization as $f(x)$. Finally, we may take a fragmentation function motivated by the notion that, since gluons are color octets, they may fragment into hadrons much more readily than quarks

$$\lim_{x\to 0} g(x) \sim 2\lim_{x\to 0} f(x),$$

but that as $x \to 1$ their fragmentation function should be suppressed by $O(\alpha_c/\pi(1-x))$ with respect to the quark fragmentation function. A simple function satisfying these criteria, and with a normalization $\int xg(x)\,dx \sim \frac{2}{3}$, is

$$xg(x) = 5(1-x)^7 + \tfrac{1}{15}(1-x)^2. \tag{2.13b}$$

We now calculate the three-jet angular distribution about the resulting jet axis. Following Bjorken and Brodsky,[21] the jet axis is determined by diagonalizing the sphericity tensor

$$S_{ij} = \sum_a (\delta_{ij} p_a^2 - p_{ai}p_{aj}), \tag{2.14}$$

and selecting the minimum eigenvalue, which is called the "sphericity." Here the index a runsover all the hadrons in the final state. We incorporate the sum on a into our calculation via the fragmentation functions

$$S_{ij} = \sum_k (\delta_{ij} p_k^2 - p_{ki}p_{kj})\langle x^2\rangle_k,$$

where

$$\langle x^2\rangle_k = \int_0^1 dx\, x^2 f_k(x),$$

and the index k runs over the quarks and gluons in the final state. $\langle x^2\rangle_k$ is simply an overall multiplying constant unless different quark and gluon fragmentation functions are used. In the latter case, $\langle x^2\rangle_k$ acts to skew the jet axis to be more in line with the axis of production of those constituents which fragment into particles with the greatest mean x.

We then calculate the inclusive cross section about the jet axis, $d\sigma/dx_\perp$, where $x_\perp (= 2p_\perp/Q)$ is measured with respect to the jet axis. This graph is shown in Fig. 4 for the gluon fragmentation function set equal to $f(x)$, and in Fig. 5 for $g(x)$ given by Eqs. (2.13a) and (2.13b). We have chosen Q's which bracket the center-of-mass energies to be expected from SPEAR, CESR, PEP, and PETRA, plus the possibility that the energy of the latter machines may be extended to 46 GeV. For comparison, we have included the transverse-momentum contribution of ordinary two-jet events, which we have parametrized as

$$\frac{d\sigma}{dp_\perp} = 12\langle n_{\mathrm{ch}}\rangle p_\perp e^{-6p_\perp^2}, \tag{2.15}$$

where the exponential falloff is taken from SPEAR data at 7.4 GeV.[1]

Finally, we introduce an eikonal approximation in the calculation of the hadronic part of the matrix element, by neglecting p_3 with respect to p_1 and p_2 whenever possible. In this approximation the hadronic matrix element $H_{\mu\nu}$ is

$$\frac{1}{4}H_{\mu\nu}=\frac{1}{p_1\cdot p_3}[\{p_1,p_2\}_{\mu\nu}-\{p_1,p_1\}_{\mu\nu}]+\frac{1}{p_2\cdot p_3}[\{p_1,p_2\}_{\mu\nu}-\{p_2,p_2\}_{\mu\nu}]+\frac{2p_1\cdot p_2}{(p_1\cdot p_3)(p_2\cdot p_3)}\{p_1,p_2\}_{\mu\nu}. \quad (2.16)$$

The last term dominates the expression. This gives the approximate differential cross section (where the angles ϕ, χ are integrated)

$$\frac{d\sigma}{dx_1dx_2}=\sum q_a{}^2\frac{\alpha^2\alpha_c}{8Q^2}\frac{2x_1x_2}{(1-x_1)(1-x_2)}\times(2+\sin^2\theta)d\cos\theta \quad (2.17)$$

or, integrating the angle θ,

$$\frac{1}{\sigma_{pt}}\frac{d\sigma}{dx_1dx_2}=\frac{2}{3}\frac{\alpha_c}{\pi}\frac{2x_1x_2}{(1-x_1)(1-x_2)}, \quad (2.18)$$

where a factor of 4 from color summation has been included. The differential cross section $(1/\sigma_{pt})d\sigma/dx_\perp$ obtained from this approximation is also plotted in Fig. 5 for comparison with the exact result, Eq. (2.9). We note that the eikonal approximation is quite good. We shall use this approximation later when we study the production of four jets.

In Fig. 6 we plot the angular distribution of the three jets on the jet plane.

Because of asymptotic freedom, quark-gluon coupling in QCD should be considered as a function of the energy-momentum invariants involved. However, it has been shown by EGR that such a

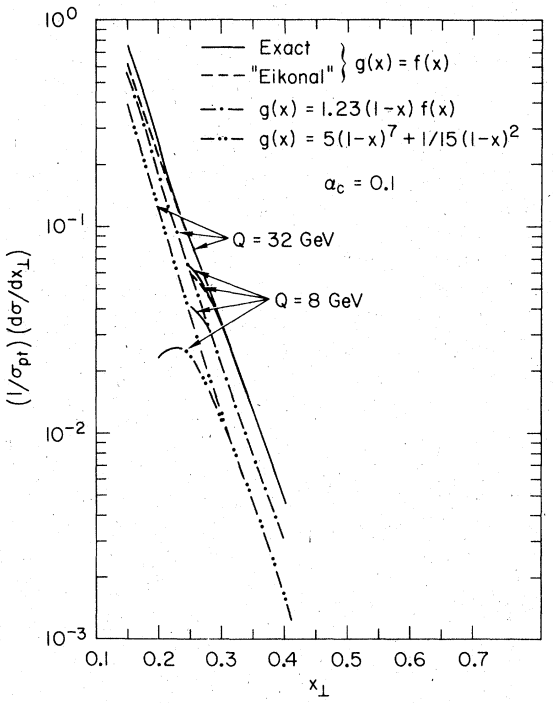

FIG. 5. $(1/\sigma_{pt})d\sigma/dx_\perp$ for $q\bar{q}G$, showing the effects of the gluon fragmentation functions (2.12) and (2.13), and of the eikonal approximation.

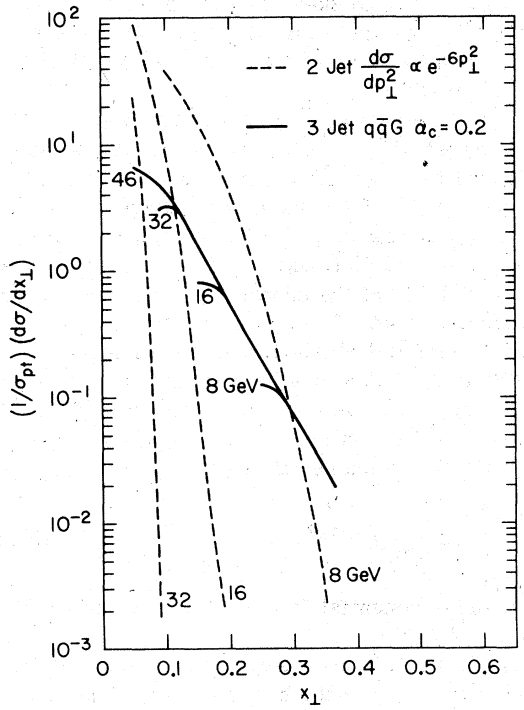

FIG. 4. Inclusive transverse distribution $(1/\sigma_{pt})d\sigma/dx_\perp$ for two jets and for $(q\bar{q}G)$ three-jet processes, with $\alpha_c = 0.2$.

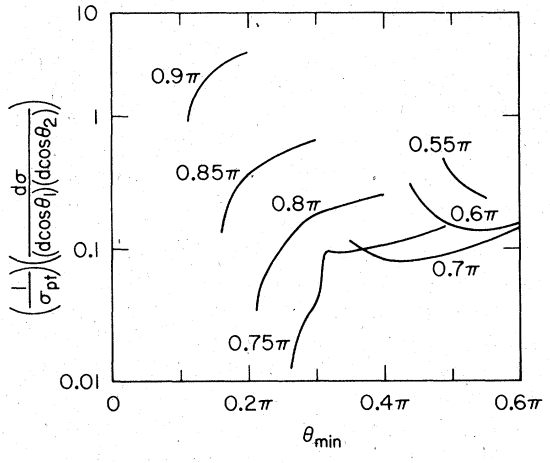

FIG. 6. $(1/\sigma_{pt})d\sigma/d\cos\theta_1 d\cos\theta_2$ plotted as a function of the smallest angle between the jets, for various values of the intermediate angle θ_{next} (which is marked on the curves) between two jets on the three-jet plane. We define $(2\pi-\theta_{next}-\theta_{min})\geq\theta_{next}\geq\theta_{min}$. Here $Q=16$ GeV, but the curves are insensitive to Q.

dependence changes little the jet structure behavior. Hence we shall simply take the color coupling α_c to be a constant throughout.

III. WIDE-ANGLE HADRON FRAGMENTATION

We turn next to another competing production process, in which a quark fragments a meson with a large transverse momentum. Of course, at small transverse momentum, the metamorphosis of a quark into hadrons is given by the fragmentation function, Eq. (2.12), where the transverse momentum is sharply (~ 0.35 GeV) cut off. However, at wide angles in various hadronic scattering processes it has been clearly demonstrated that the transverse-momentum distribution takes on a power-law behavior, and current large-angle scattering data are quite successfully described by the constituent-interchange model (CIM) and dimensional counting.[19] Following the CIM prescription and dimensional counting, we obtain the Q^2 behavior of the meson-emission process of Figs. 7(a) and 7(b).

$$\frac{1}{\sigma_{\rm pt}}\frac{d\sigma(q\bar{q}\pi)}{dx_1 dx_2}\sim\frac{1}{Q^2}f(x_1,x_2), \tag{3.1}$$

where x_1 and x_2 are, as given before,

$$s_{13}=(p_1+p_3)^2=Q^2(1-x_2), \tag{3.2a}$$

$$s_{23}=(p_2+p_3)^2=Q^2(1-x_1). \tag{3.2b}$$

In comparison, the three-jet process has the scaling behavior

$$\frac{1}{\sigma_{\rm pt}}\frac{d\sigma(q\bar{q}G)}{dx_1 dx_2}\sim g(x_1,x_2). \tag{3.3}$$

To calculate the meson-emission process, we use the method of the CIM. In that spirit, we use ϕ^4 theory and neglect the interference term between the two graphs of Figs 7(c) and 7(d). The quarks are taken to be scalar fields and the meson is taken to be a bound state of scalar fields. Thus the differential cross section is given by[22]

$$\begin{aligned}d\sigma=&\frac{1}{2Q^2}\left[\prod_{i=1}^{4}\frac{d^4k_i}{(2\pi)^3}\delta^+(k_i^2-\mu^2)\right]\delta^+((k_2+k_3)^2-m^2)\\&\times(2\pi)^4\delta^4(Q-k_1-k_2-k_3-k_4)q_a^2e^4g^2\\&\times\left\{\frac{8k_1\cdot p_a k_1\cdot p_b}{Q^4[(Q-k_1)^2-\mu^2]^2}+\frac{8k_4\cdot p_a k_4\cdot p_b}{Q^4[(Q-k_4)^2-\mu^2]^2}\right\},\end{aligned} \tag{3.4}$$

where the photon–scalar-field coupling is used instead of the photon–spinor-field coupling for the quark-photon vertex. Since k_2+k_3 is the four-momentum of the meson, it is most convenient to introduce

$$1=\delta^4(k_2+k_3-p)\,d^4p \tag{3.5}$$

and integrate over k_2 and k_3. For our purposes, the quark mass μ and the meson mass m are both negligible. Using the formula

$$\int d^4k_2 d^4k_3\delta^+(k_2^2-\mu^2)\delta^+(k_3^2-\mu^2)\delta^4(k_2+k_3-p)=\tfrac{1}{2}\pi \tag{3.6}$$

and

$$\int d^4p\,\delta^+(p^2-m^2)\delta^4(Q-k_1-k_2-p)\simeq\delta^+((Q-k_1-k_2)^2), \tag{3.7}$$

we obtain

$$d\sigma\sim\frac{1}{(2\pi)^8}q_a^2e^4g^2\frac{2\pi}{Q^6}\int d^4k_1\,d^4k_4\,\delta^+(k_1^2)\delta^+(k_4^2)\delta^+((Q-k_1-k_4)^2)\delta^+((Q-k_1)^2-s_{13})\delta^+((Q-k_4)^2-s_{23})ds_{13}\,ds_{23}$$
$$\times\left(\frac{k_1\cdot p_a k_1\cdot p_b}{s_{13}^2}+\frac{k_4\cdot p_a k_4\cdot p_b}{s_{23}^2}\right), \tag{3.8}$$

where we have introduced

$$1=\delta^+((Q-k_1)^2-s_{13})ds_{13} \tag{3.9}$$

and similarly for s_{23}. Integrating k_1 and k_4 gives the cross section we want. Note that the interference term between the two graphs of Figs. 7(c) and 7(d) is neglected. Let us consider the first term of Eq. (3.8). It can be written as

$$\theta=p_{a\mu}p_{a\nu}\theta_{\mu\nu}\frac{1}{(2\pi)^8}q_a^2e^4g^2\frac{2\pi}{Q^6}\frac{1}{s_{13}^2}$$

so that $\theta_{\mu\nu}$ must be of the form

$$\theta_{\mu\nu}=Q_\mu Q_\nu I_1+g_{\mu\nu}I_2. \tag{3.10}$$

Contracting this with $Q^\mu Q^\nu$ and $g^{\mu\nu}$ gives [$k_i\cdot Q=(Q^2-s_{13})/2$]

$$Q^4I_1+Q^2I_2=(Q^2-s_{13})^2\tfrac{1}{4}I, \tag{3.11a}$$

$$Q^2I_1+4I_2=0, \tag{3.11b}$$

so that

$$\theta=(p_a\cdot Q\,p_b\cdot Q-\tfrac{1}{4}Q^2p_a\cdot p_b)\frac{(Q^2-s_{13})^3}{3Q^4}I$$
$$=\tfrac{1}{24}(Q^2-s_{13})^2I, \tag{3.12}$$

where

$$I=\int d^4k_1 d^4k_4 \delta^+(k_1^2-\mu^2)\delta^+(k_4^2-\mu^2) \times \delta^+((Q-k_1-k_4)^2-m^2)\delta^+((Q-k_1)^2-s_{13}) \times \delta^+((Q-k_4)^2-s_{23}). \quad (3.13)$$

To evaluate Eq. (3.13) we first integrate k_1 in the $\vec{Q}=0$ frame. Then

$$I=\int d^4k_4 \delta^+(k_4^2-\mu^2)\delta^+((Q-k_4)^2-s_{23})\frac{\pi}{4}\frac{1}{Q\cdot k_4} = \frac{\pi^2}{4}\frac{1}{Q^2}. \quad (3.14)$$

Evaluating the second term of Eq. (3.8) in the same way, we obtain the cross section for meson emission

$$\frac{d\sigma}{ds_{13}ds_{23}} = \frac{1}{3}\frac{q_a^2\alpha^2}{(16\pi)}\left(\frac{g}{4\pi}\right)^2\frac{1}{Q^8} \times\left[\frac{(Q^2-s_{13})^2}{s_{13}^2}+\frac{(Q^2-s_{23})^2}{s_{23}^2}\right]. \quad (3.15)$$

Summing over the electric charges and color and spin factors, and using Eq. (3.2), we obtain

$$\frac{1}{\sigma_{pt}}\frac{d\sigma}{dx_1dx_2} = \frac{1}{16\pi^2}\left(\frac{g}{4\pi}\right)^2\frac{1}{Q^2}\left[\frac{x_2^2}{(1-x_2)^2}+\frac{x_1^2}{(1-x_1)^2}\right]. \quad (3.16)$$

This is of the form given by Eq. (3.1). The absence of an (x_1, x_2) mixing term in Eq. (3.16) is due to the exclusion of the interference term. Integrating s_{23} in Eq. (3.15) gives

$$\frac{d\sigma}{ds_{13}} \propto \frac{\epsilon^2}{Q^2 s_{13}^2}, \quad \epsilon = 1-\frac{s_{13}}{Q^2}, \quad (3.17)$$

in agreement with the CIM counting rules. For high enough energy, this process will be suppressed with respect to the gluon bremsstrahlung process (2.9) by the $1/Q^2$.

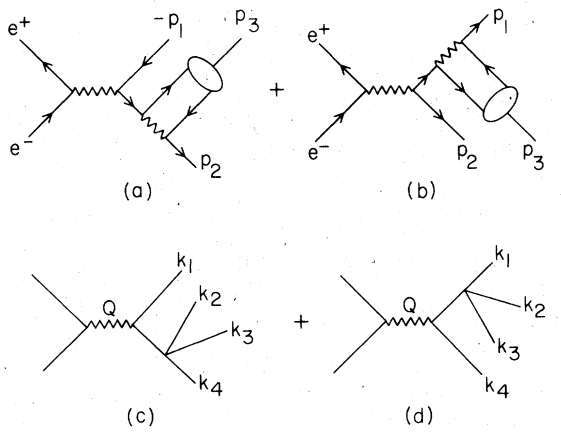

FIG. 7. The pion-emission subprocess. In (a), (b), p_3 is the momentum of the pion. Our calculation is actually based on ϕ^4 theory, (c), (d), where the pion momentum is k_2+k_3.

To find out the importance of this process, we have to normalize it properly. We shall discuss two ways of doing this.

(1) $(g/4\pi)^2$ can be extracted from other experiments using the CIM approach. The quark-quark-meson vertex coupling has been extracted from data to be[23]

$$\frac{1}{4\pi}\left(\frac{g}{4\pi}\right)^2_{\text{bare}} \sim 2\ \text{GeV}^2. \quad (3.18)$$

For our purpose, we must include the probability that some of the mesons produced may come from decays of higher resonances. This increases the basic coupling (3.18) by approximately a factor of 3.[23] In addition we should add the probability of the production of mesons via the sea quarks. This is estimated to give an extra factor of 3. Putting them all together we extract the value for the final effective quark-meson coupling

$$\left(\frac{g}{4\pi}\right)^2_{\text{effective}} \simeq 220\ \text{GeV}^2. \quad (3.19)$$

This is an order of magnitude estimate.

(2) An upper bound on the quark-meson coupling $(g/4\pi)^2$ can be obtained by requiring that the CIM process be consistent with SPEAR data at 7.4 GeV. We show a plot (Fig. 8) comparing the data, which has a $p_\perp$ behavior that is consistent with

$$\frac{d\sigma}{dp_\perp^2} \sim e^{-6p_\perp^2}$$

and the CIM process, normalized according to Eq. (3.19). We see that this normalization is consistent with the data, although the error bars are quite large. If a reanalysis of SPEAR data can shrink the error bars on the large-$p_\perp$ data points, we will have a very clear normalization on the coupling constant of the CIM, or at least an upper limit on its value. At present, however, we can only say that the data and our CIM normalization are consistent with one another. We can consider this as an upper bound.

We shall take the coupling strength normalized by Eq. (3.19) and compare the CIM process to the gluon bremsstrahlung process. This is given in Fig. 9. Notice that the gluon bremsstrahlung cross section is overwhelmed by the CIM process at $Q=8$ GeV but becomes important as Q increases. At $Q=32$ GeV, the gluonic process may be the dominant process at $x_\perp > 0.2$ if the effective α_c is not too small (i.e., $\alpha_c \gtrsim 0.20$). Irrespective of the actual size of α_c, we believe both processes are not negligible at all PEP and PETRA energies (i.e., $Q \leq 32$ GeV). The difficult task is to pick out

the gluonic events, since experimentally both have a three-jet–like structure. We summarize the various possible approaches as follows:

(1) Search for an angular dependence of the normal of the three-jet plane with respect to the e^+e^- direction. For gluon bremsstrahlung processes, this is proportional to $2+\sin^2\theta$.

(2) The angular distribution of the three jets for the gluon bremsstrahlung on the jet plane is given in Fig. 6.

(3) For fixed large $x_\perp$ (i.e., $x_\perp > 0.2$), we parametrize the cross section by

$$\frac{1}{\sigma_{pt}}\frac{d\sigma}{dx_\perp}(Q^2) = A + \frac{B}{Q^2} + \frac{C}{Q^4} + \cdots . \tag{3.20}$$

Varying Q^2, we can deduce the value of A. $A \neq 0$ indicates a gluonic piece.

(4) Alternatively we can also fix the angles for three jets or the two jets plus the meson (i.e., CIM process) and measure this differential cross section as a function of Q^2 to pick out the gluonic piece. The three solid angles must be coplanar,

$$\frac{1}{\sigma_{pt}}\frac{d\sigma}{d\Omega_1 d\Omega_2 d\Omega_3} = a + \frac{b}{Q^2} + \cdots , \tag{3.21}$$

$a \neq 0$ indicates a gluonic piece.

(5) It may be possible to eliminate more CIM events in comparison to the gluonic events by putting a cutoff on the x_{max} of the leading particles, say $x_{max} < 0.6$. This may be useful since we expect the meson to carry practically all the momentum of hadrons coming out in its direction while the gluon may prefer to fragment into wee hadrons [recall Eq. (2.13)].

(6) Events with a gluonic jet may have a much higher multiplicity than two-jet events. This is because gluons are color octets. The system of a gluon (an octet) moving apart from a $q\bar{q}$ pair (also an octet) possesses a larger net charge separation than a quark (a color triplet) separating from an antiquark (also a triplet). The larger charge separation may be reflected in a larger multiplicity of final-state hadrons; for color SU(3), the fractional increase over ordinary two-jet events is $\frac{9}{4}$.[20] So it may be possible to identify events with gluonic jets by selecting events with larger-than-average multiplicity for analysis.

(7) Finally, one may be able to differentiate between the different kinds of jets by measuring correlations between the particles produced in the fragmentations of the jets. Here again, comparison with lower SPEAR energies will be important. If we can see definite three-jet events at CESR, PEP, or PETRA, we expect that two of the jets (arising from quark fragmentation) will have properties similar to the quark jets seen at SPEAR.

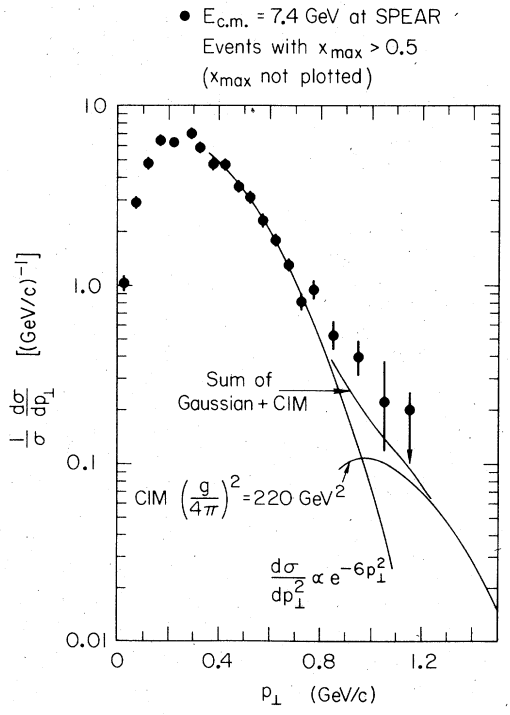

FIG. 8. Normalization of the CIM process as compared to the data from SPEAR at $Q = 7.4$ GeV. Data are taken from Ref. 1.

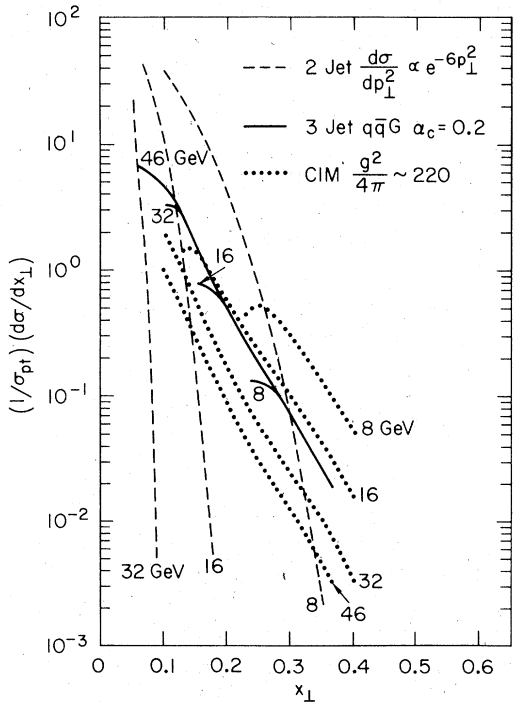

FIG. 9. The transverse-momentum distribution for two-jet, three-jet, and CIM processes.

If the third jet arises from the decay of a CIM-produced meson, then we expect its distribution of final-state hadrons to be characteristic of "typical" resonance decay, and calculable, for instance, by Monte Carlo methods. If the third jet is gluonic, we expect a rather different behavior, since gluons are flavor SU(3) singlets. For instance, the mean charge of particles in the gluon jet should be zero. There should be some correlations in rapidity between, say, leading K^+'s and K^-'s in the gluon jet, since the leading K's will have been produced half the time from the annihilation of the gluon into an $s\bar{s}$ quark pair, which then decay into kaons. Finally, we expect flavor correlations between the leading particles of two of the jets if the third jet arises from gluons; these particles are formed from the fragmentation of the original $q\bar{q}$ pair produced by the photon. As meson emission in the manner of CIM also implies flavor transformation of quarks, quantum numbers need not be conserved so strongly between the leading particles of different jets.

IV. FOUR-JET STRUCTURE

As we have seen, the angular distribution of the three-jet plane with respect to the e^-e^+ direction and the angular distribution of the three jets on the jet plane provide important signals for the three-jet structure against the background due to the CIM process. In this section we examine the contribution to large-$p_\perp$ meson production due to the emission of four jets. This will give some indication of the relative significance of multiple-bremsstrahlung processes. Based on our calculations we conclude that at the upper range of PEP/PETRA energies the four-jet cross section is a fair-sized fraction of the three-jet cross section. For large $x_\perp$ and at large energies the four-jet structure will also dominate over the CIM process. If the cross section is parametrized as in Eq. (3.21), the scaling piece of $(1/\sigma_{\rm pt})d\sigma/dx_\perp$ will receive further contributions from the four-jet structure, and, for that matter, it will also receive contributions from higher multiple-bremsstrahlung processes. Now we outline our four-jet calculations

There are two types of processes which may produce events with four hadronic jets: (1) $e^+e^- \to \gamma \to q\bar{q}\,q\bar{q}$, and (2) $e^+e^- \to \gamma \to q\bar{q}GG$ as shown in Fig. 10. They are of order $O(\alpha_c^2)$. We shall only be interested in the qualitative behavior of the four-jet structure and its size in comparison to the three-jet process. Thus it suffices for us to study a small set of Feynman graphs which, by itself, is gauge invariant and gives a positive-definite contribution to the four-jet cross section. We shall consider, for simplicity, the process $e^+e^- \to \gamma \to (q\bar{q})(q\bar{q})$, where the two quark pairs are of different flavors. This clearly gives a lower bound to the four-jet process. No knowledge of the gluon fragmentation function is required here. Even for this process, the calculation is nontrivial. In what follows we content ourselves by studying only the most logarithmically divergent terms.

The calculational procedure is similar to the three-jet case. Throughout the calculation we suppose the quarks and gluons to be effectively massless. Denote the momenta of the incoming electron and positron by q_1 and q_2, and those of the outgoing quark-antiquark pair of flavor a and b by p_i, $i=1$, 4, (2, 3) for a (b) quark and $\bar{a}$ ($\bar{b}$) quark, respectively, as shown in Fig. 11. The differential cross section is given by

$$d\sigma = (2\pi)^4\delta^4(q-p_1-p_2-p_3-p_4)\left(\prod_{i=1}^{4}\frac{d^3p_i}{(2\pi)^3 2E_i}\right) \times \frac{1}{2Q^2}|T|^2, \tag{4.1}$$

where

$$T = \frac{e^2g^2}{Q^2}\bar{v}(q_2)\gamma^\mu u(q_1)\left\{\frac{-q_a}{s_{23}s_{234}}\bar{u}(p_1)\gamma_\mu \not{p}_{234}\gamma^\alpha v(p_4)\bar{u}(p_3)\gamma_\alpha v(p_2) + \frac{q_a}{s_{23}s_{123}}\bar{u}(p_1)\gamma^\alpha \not{p}_{123}\gamma_\mu v(p_4)\bar{u}(p_3)\gamma_\alpha v(p_2) - \frac{q_b}{s_{14}s_{124}}\bar{u}(p_3)\gamma_\mu \not{p}_{124}\gamma^\alpha v(p_2)\bar{u}(p_1)\gamma_\alpha v(p_4) + \frac{q_b}{s_{14}s_{134}}\bar{u}(p_3)\gamma^\alpha \not{p}_{134}\gamma_\mu v(p_2)\bar{u}(p_1)\gamma_\alpha v(p_4)\right\}, \tag{4.2}$$

with q_a (q_b) denoting the fraction of a (b) quark electric charge, and

$$p_{ij}=p_i+p_j, \quad p_{ijk}=p_i+p_j+p_k, \quad s_{ij}=p_{ij}^2, \quad s_{ijk}=p_{ijk}^2. \tag{4.3}$$

The computational details are relegated to Appendix B. For the differential cross section in Eq. (4.1) we average over initial polarizations and sum over the final polarizations. We include the processes where the a and b quarks are different. For the same-flavor quark pairs, the interference term in $|T|^2$ is rather complicated and we have not calculated it. Here we apply the eikonal approximation that is used for the three-jet case (see Fig. 5 and Sec. II) to the scattering amplitude

(4.2). Again we restrict ourselves to study the kinematical region where asymptotic freedom and perturbative calculations are applicable, namely, all invariants $s_{ij}, s_{ijk} > 10$ GeV^2. Since all jets arise from fast quarks, we can safely employ the fragmentation function (2.12). The jet axis is found employing the same method for the two-jet process. The inclusive cross section $(1/\sigma_{pt})d\sigma/dx_\perp$ with respect to the jet axis is plotted in Fig. 12. The slowness of the approach to scaling in the region $Q \lesssim 32$ GeV is due to our kinematic cuts $s_{ij}, s_{ijk} > 10$ GeV^2. We repeat that this is the lower bound of the four-jet process, since processes of Fig. 10(b)–10(d) are not included (also excluded is the same-quark-pairs case).

So far we have assumed that a hard gluon fragments in a similar fashion as energetic quark. If this is not the case, it is possible for the transverse-momentum distribution of the three-jet process to be much narrower. From Fig. 12 it is clear that the four-jet structure will dominate (over the CIM process) for large $x_\perp$ provided Q^2 is large enough. However, barring the above unlikely possibility, the three-jet structure will be dominant for large $x_\perp$ at the highest PEP and PETRA energies.

In the eikonal approximation, we can also integrate analytically the four-jet cross section (N is the number of flavors)

$$\frac{\sigma_{4\,\mathrm{jet}}}{\sigma_{pt}} > \frac{8\alpha_c^{\,2}}{9\pi^2}(N-1)\left(\sum q_a^{\,2}\right)\left(|\ln\epsilon|^3 + O|\ln\epsilon|^2\right)$$

(where $\epsilon = Q_0^{\,2}/Q^2$), or

$$\sigma_{4\,\mathrm{jet}}/\sigma_{3\,\mathrm{jet}} > \tfrac{2}{3}(N-1)\frac{\alpha_c}{\pi}|\ln\epsilon|.$$

At $Q = 32$ GeV, for example, this ratio is about $\frac{1}{2}$ if we take $\alpha_c \sim 0.2$, $Q_0^{\,2} \sim 10$ GeV^2, and $N = 4$.

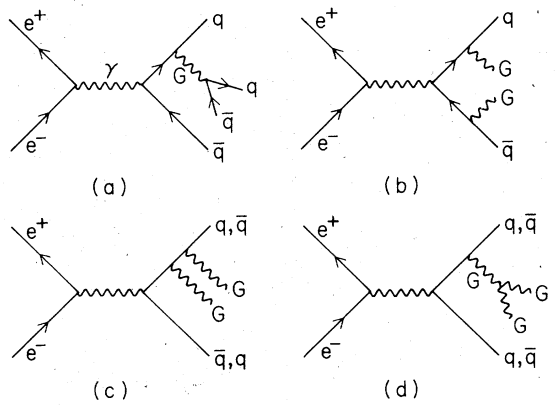

FIG. 10. The subprocesses that contribute to four-jet structures.

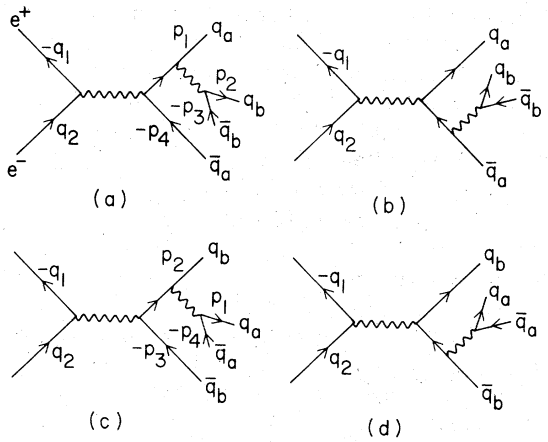

FIG. 11. The subprocesses that give four-quark–jet structure. We consider only these diagrams.

V. JETS AND HEAVY-QUARK RESONANCES

So far we have considered only processes that are of the order $O(\alpha_c)$ and $O(\alpha_c^{\,2})$. In general, processes that are of higher order in α_c are less amenable to computation and harder to investigate. One known exception would arise if there exist new heavy quarks,[24] more massive than the

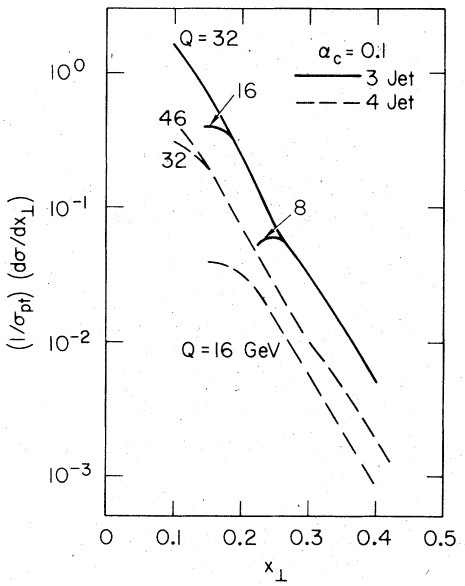

FIG. 12. The four-quark–jet cross section in comparison to the three-jet cross sections ($\alpha_c = 0.1$). Recall that the four-jet curves shown here give only a lower bound on the cross section. Notice the slow approach to scaling in the region $Q \lesssim 32$ GeV owing to our kinematic cuts.

charmed quark. If another quark of mass m is found in e^+e^- annihilation, then the ground-state meson which is the analog of the ψ will have a mass of about $2m$. In QCD, the hadronic decay of such a state proceeds via a three-gluon intermediate state. Hence, if the new resonance is very massive, every hadronic decay should be, at least in principle, a three-jet event, for each gluon is *a priori* sufficiently energetic to decay into a large number of hadrons.

One might expect that the same statement could be made for the decays of the ψ, since in the QCD picture its decay is also mediated by a three-gluon intermediate state. But events resembling three jets are not seen in the decays of the ψ. That is because the mass of the ψ is so low that the average energy of a gluon in its decay is roughly 1 GeV. We know that quark jets become observable only when the center-of-mass energies are bigger than 5 GeV, that is, for quark energies greater than about 2 to 3 GeV. We expect that jet structure in the decay of the new resonance should become prominent should the average gluon energy be greater than 3 GeV; hence if $\frac{2}{3}m$ is bigger than 3 GeV or so, the decays of the new state via three-jet events should be dominant.

The differential decay rate of the new resonance can easily be obtained since it is exactly the analog of the decay of orthopositronium into three photons. The leptonic width of the new state is given by

$$\Gamma(q\bar{q}\to e^+e^-)=2\pi\alpha^2 q_a{}^2\left(\frac{4}{3}\right)^2\frac{Q^2+2m^2}{Q^4}\left|\psi(0)\right|^2, \tag{5.1}$$

where the charge of the new quark is q_a, m is the mass of the quark and $\psi(0)$ is the bound-state wave function at the origin. At resonance $Q^2\sim 4m^2$,

$$\Gamma(q\bar{q}\to e^+e^-)\sim\frac{16}{3}\frac{\pi\alpha^2}{Q^2}q_a{}^2\left|\psi(0)\right|^2. \tag{5.2}$$

The hadronic decay rate via 3 gluons is given by

$$\Gamma(q\bar{q}\to 3g)=\frac{16}{9}(\pi^2-9)\frac{4\alpha_c{}^2}{Q^2}\frac{5}{18}\left|\psi(0)\right|^2, \tag{5.3}$$

while the differential hadronic rate is given by

$$\frac{d\Gamma_{3g}}{ds_{13}ds_{23}}=4\frac{16}{9Q^2}\alpha_c{}^3\frac{5}{18}\left|\psi(0)\right|^2 \times\left\{\left[\frac{Q^2-s_{13}-s_{23}}{(Q^2-s_{13})(Q^2-s_{23})}\right]^2+\text{permutations}\right\} \tag{5.4}$$

or, in terms of x_1, x_2,

$$\frac{d\Gamma_{3g}}{dx_1dx_2}=\frac{160}{81}\frac{\alpha_c{}^3}{Q^2}\left|\psi(0)\right|^2 \times\left\{\left(\frac{1-x_3}{x_1x_2}\right)^2+\text{permutations}\right\}. \tag{5.5}$$

The cross section at the resonance peak is given by

$$\frac{d\sigma}{dx_1dx_2}=\frac{12\pi}{Q^2}\frac{\Gamma_{e^+e^-}}{\Gamma_t{}^2}\frac{d\Gamma_{3g}}{dx_1dx_2}, \tag{5.6}$$

where Γ_t is the total width.

We may perform the usual jet-finding analysis which was applied to the three-jet events of Secs. II and III to the decays of these bound states. In Fig. 13 we graph the distribution $(1/\Gamma_{3g})d\Gamma/dx_\perp$ of hadrons about the jet axis, using the two gluon fragmentation functions (2.12) and (2.13).

In Fig. 14 we plot the cross section $d\Gamma/d\Omega_1 d\Omega_2$ of the three gluons in their plane.

In the quark-confining string, the hadronic decays of the new resonance take place as shown in Fig. 15. The Zweig-Okubo-Iizuka rule is explicit in this diagrammatic form; in Fig. 15(a), the decay goes via a closed string, which resembles a virtual photon, in the sense that such a closed

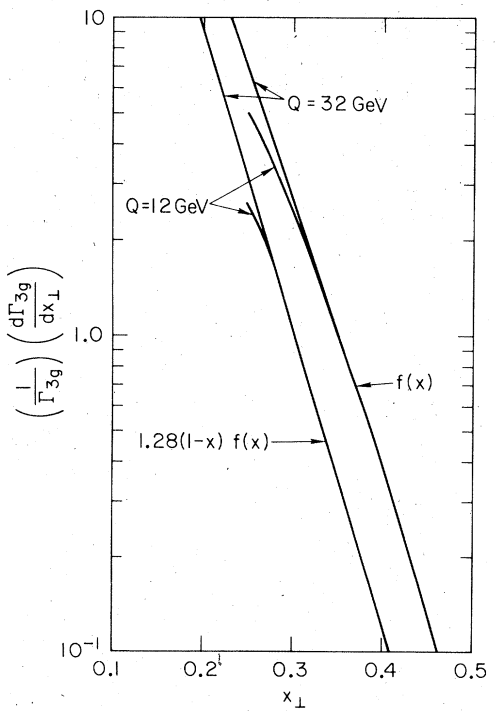

FIG. 13. The transverse-momentum distribution of the decay of a bound state $(q\bar{q})$ of heavy quark q. The jet axis is defined as the minimum-$p_\perp$ axis.

string cannot be a physical state (see Appendix A). The closed string fragments into a number of hadrons and the distinct three-jet structure present in QCD is completely absent here. If the ordinary dual model is any guide to the phenomenology of the QCS, one expects in this picture either a broadened two-jet structure from the decay of the heavy meson *or* an approximately isotropic distribution.

Hence if another heavy quark exists, observation of three distinct jets in the decays of its ψ-like bound state will be a very clean indication of the existence of gluons. If gluon jets are produced, the mean sphericity of events should show a marked deviation as one tunes through the resonance peak. The decay angular distribution of Eq. (5.5) has an average sphericity

$$\langle s\rangle = \frac{3\left(\sum_i p_{\perp i}^2\right)_{\min}}{2\sum_i p_i^2} = 0.23$$

in contrast to the somewhat lower values ($\langle s\rangle \sim 0.08$) seen away from resonance peak, where jet production is dominated by the nonresonant process of Secs. II–IV.

If quarkless states exist in QCD, the three-jet structure from the decay provides a very good place to search for them. One expects the gluons to be inclined to form quarkless states, especially as the leading particles of the gluonic jets.

Finally, should three-jet events be observed, this will be a good place to study the gluon fragmentation function. Since gluons are color octets and quarks are triplets, and a system of octets moving apart from each other corresponds to a greater net color separation than a system of triplets moving apart, we may speculate that the confining force may produce a higher multiplicity of hadrons in the final state when gluons separate than when quarks separate. If this is true, we may expect to see a rise in multiplicity as we tune through the new resonance.

Clearly, should a new massive narrow resonance be found, it will be a most important laboratory for the study of the dynamics of hadron interactions. (See note added in proof.)

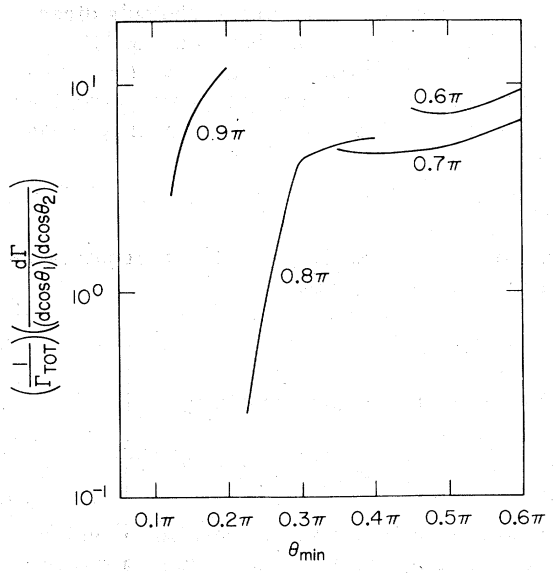

FIG. 14. The angular distribution of the three jets on the three-jet plane of the bound state. The three angles between the jets are $(2\pi - \theta_{\text{next}} - \theta_{\min}) \geq \theta_{\text{next}} \geq \theta_{\min}$. The x axis is $\theta_{\min}$. θ_{next} is marked on each curve.

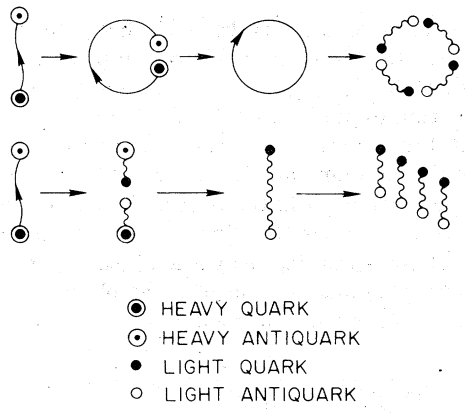

FIG. 15. The schematic picture of the decay of a bound state of heavy-quark-antiquark to usual mesons of light quarks (i.e., u, d, s, c quarks) in the QCS picture. The closed loop is a virtual intermediate state. The wavy lines indicate possible presence of string excitation modes in the hadrons.

VI. JET STRUCTURE IN DEEP-INELASTIC ELECTROPRODUCTION

So far we have considered the jet structure in e^+e^- annihilation. As is obvious, a similar jet structure is expected in deep-inelastic electroproduction. In this section we briefly compare the broadening of jet structure in deep-inelastic lepton-proton scattering due to gluon or pion emission to that expected in e^+e^- annihilation.

The lowest-order process $l^- + p \to l^- + h + X$ proceeds via the collision of a virtual photon with one of the quarks in the proton, followed by the scale-invariant fragmentation of that quark into the final-state hadron h [Fig. 16(a)]. In the scaling region[2]

$$\frac{d\sigma}{dQ^2 d\nu dy} = \frac{4\pi\alpha^2}{Q^4\nu}\left(1 - \frac{\nu}{E} + \frac{\nu^2}{2E^2}\right) \times \sum_i F_{i/p}\left(\frac{Q^2}{2M\nu}\right) f_{h/i}(y), \tag{6.1}$$

where E is the energy of the incoming lepton in the lab frame, the invariant mass of the photon is $q^2=-Q^2$, $2M\nu=2p_{\text{proton}}\cdot q$, $f_{i/j}(x)$ is the fragmentation function to produce particle i from constituent j, $F_{i/p}(x)$ is the structure function for constituent i in the proton [normalized so that $F(x)=\nu W_2(x)$], and $y=p/\nu$, where p is the longitudinal momentum of the hadron h along the direction of the virtual photon. Upon summing over h and assuming that $\sum_h f_{h/i}(y)=f(y)$ independent of i, we obtain the distribution of energetic hadrons

$$\frac{dN}{dy}=\left(\frac{d\sigma}{dQ^2d\nu}\right)^{-1}\frac{d\sigma}{dQ^2d\nu dy}=f(y), \tag{6.2}$$

which is the same fragmentation that appears in e^+e^- annihilation.[25] Again we have assumed a sharp cutoff in momentum transverse to the virtual photon's direction.

We now estimate the broadening of the jet structure due to gluon bremsstrahlung and pion emission [Figs. 16(b)–16(e)]. We should include contributions to jet broadening in which the initial parton in the proton is a gluon [Fig. 16(f), for example], since in QCD, gluons carry roughly half the momentum of the proton in the infinite-momentum frame; but due to our ignorance of the gluon structure function, we shall ignore them. We shall also use the eikonal approximation, so that our results give only an order of magnitude estimate of the gluon bremsstrahlung and CIM processes in deep-inelastic lepton-hadron scattering. A more detailed and slightly different analysis has been given by Floratos.[15]

First, let us consider the pion-emission subprocess [Fig. 17(a)]. The differential cross section is given by

$$d\sigma=\frac{d^3p_3}{2E_3}\frac{d^3p_2}{2E_2}\frac{d^3k}{2E_k}\frac{1}{(2\pi)^5}\delta^4(p_1+q-p_2-k)\frac{1}{4p_1\cdot(q+p_3)}\frac{1}{2}\frac{q_a^2e^4}{Q^4}\left(\frac{g}{4\pi}\right)^2\left[\frac{1}{(k\cdot p_1)^2}+\frac{1}{(k\cdot p_2)^2}\right]$$
$$\times(q+2p_1)_\mu(q+2p_2)_\nu\{p_3,q+p_3\}^{\mu\nu}, \tag{6.3}$$

where scalar quarks are assumed. Using the method of Berman, Bjorken, and Kogut,[26] it is straightforward to extract the cross section for the production of a large-p_T pion from (6.3). We obtain

$$\frac{d\sigma(l+p\to l+\pi+X)}{dQ^2d\nu dyd\cos\theta}=\left[\frac{d\sigma(l+p\to l+X)}{dQ^2d\nu}\right]\left(\frac{g}{4\pi}\right)^2\frac{1}{32\pi^2}$$
$$\times\left[\frac{F(\tilde{x}(1))}{F(x)}\frac{1-y}{y}\left(\frac{1}{(Mx+yw)^2}+\frac{1}{(Mx+w)^2}\right)\right.$$
$$\left.+\int_0^1\frac{dz}{z^2}G_{\pi/q}(z)\frac{F(\tilde{x}(z))}{F(x)}\left(\frac{y/z}{(1-y/z)(Mx+wy/z)^2}+\frac{1-y/z}{(y/z)(Mx+w)^2}\right)\right], \tag{6.4}$$

where the pion is emitted with energy νy $(0<y<1)$ and angle θ with respect to the virtual photon's direction. The first term in the square brackets in (6.4) represents the emission of an observed pion [Fig. 16(b)]; the second term represents the effect of the emission of a pion from the quark, which is not observed, followed by the recoil of the quark and subsequent emission of a pion along the quark's direction of motion via scale-invariant fragmentation [Fig. 16(c)]. The fragmentation function of particle type i is $f(z)=G_{\pi/i}(z)/z$, and

$$x=Q^2/2M\nu,\quad \tilde{x}(z)=\frac{Q^2+2w\nu y/z}{2M\nu(1-y/z)},\quad w=\nu-(\nu^2+Q^2)^{1/2}\cos\theta. \tag{6.5}$$

M is the mass of the proton, taken to be 1 GeV. Notice that the proper normalization of (6.4) requires the use of scalar quarks for the deep-inelastic cross section itself. This is given by

$$\frac{d\sigma}{dQ^2d\nu}=\frac{4\pi\alpha^2}{Q^4\nu}\left(\sum_a q_a^2\right)\left(1-\frac{\nu}{E}\right)F(x). \tag{6.6}$$

The subprocess for gluonic bremsstrahlung [Fig. 17(b)] is, in the eikonal approximation,

$$d\sigma=\frac{d^3p_3}{2E_3}\frac{d^3p_2}{2E_2}\frac{d^3k}{2E_k}\frac{1}{(2\pi)^5}\delta^4(q+p_1-k-p_2)\frac{1}{4p_1\cdot(p_3+q)}q_a^2\frac{64\pi^3\alpha^2\alpha_c}{Q^4}\frac{2p_1\cdot p_2}{p_1\cdot kp_2\cdot k}16\{p_3,p_3+q\}^{\mu\nu}\{p_1,p_1+q\}_{\mu\nu}. \tag{6.7}$$

We can fold in the initial- and final-state fragmentation functions and evaluate the expression in the lab frame. The cross section for producing a pion with momentum νy at an angle θ to the virtual photon is given by

$$\frac{d\sigma}{dQ^2d\nu\,dy\,d\cos\theta}=\left(\frac{d\sigma}{dQ^2d\nu}\right)\frac{4}{3}\frac{\alpha_c}{\pi}\frac{\nu}{Mx+w}\int\frac{dz}{z^2}\frac{F(\tilde{x}(z))}{F(x)}\left[\frac{y/z}{1-y/z}G_{\pi/q}(z)+\frac{1-y/z}{y/z}G_{\pi/g}(z)\right]\frac{2E(E-\nu)+\nu^2x/\tilde{x}(z)}{2E(E-\nu)+\nu^2}, \tag{6.8}$$

where x, $\tilde{x}(z)$, and w are defined in Eq. (6.5). The first term in the square brackets represents fragmentation of the meson from the quark [Fig. 16(d)], the second term represents fragmentation from the gluon [Fig. 16(e)].

Using the fragmentation function (2.12), the CIM coupling strength (3.19), $\alpha_c \sim 0.2$, and any fit to νW_2,[27] we can calculate the broadening of the transverse distribution $dN/dx_\perp$. For the lowest-order deep-inelastic cross section, we assume an exponential transverse-momentum cutoff

$$\frac{dN}{dp_\perp{}^2} = 6\langle n_{\text{charged}}\rangle e^{-6p_\perp{}^2}.$$

In Fig. 18 we plot the various transverse distributions at $E = 145$ GeV, $\nu = 45$, 85 GeV, and $Q^2 = 15$ GeV^2, typical of Fermilab energies. We also plot them at $E = 350$ GeV, $\nu = 210$ GeV, and $Q^2 = 25$ GeV^2, which may be reached by SPS at CERN and/or the doubler at Fermilab.

The process of Fig. 16(f) clearly will enhance the contribution of the broadening due to the presence of gluonic degrees of freedom. However,

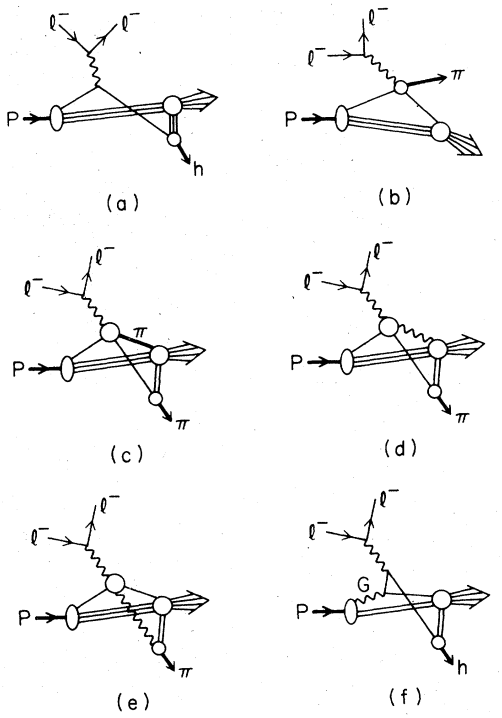

FIG. 16. Processes contributing to jet structure in lepton-hadron scattering: (a) lowest-order reaction, and jet broadening by (b) pion emission, (c) recoil of the quark after pion emission, followed by quark fragmentation, (d) gluon bremsstrahlung and quark fragmentation, (e) gluon bremsstrahlung and gluon fragmentation, (f) scattering off the gluonic component of the proton.

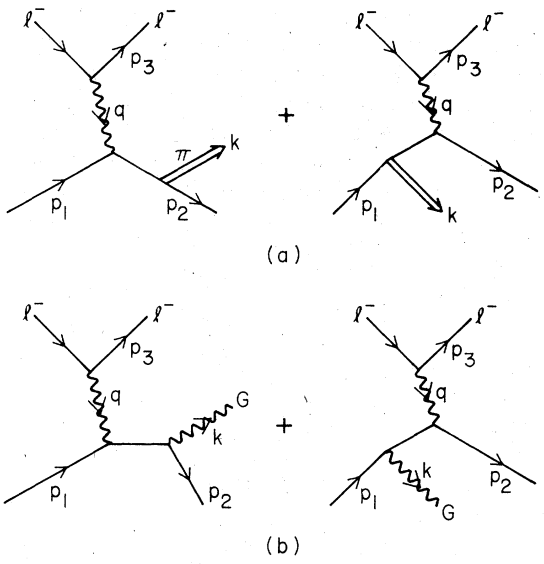

FIG. 17. The subprocesses studied in deep-inelastic scattering: (a) pion emission, (b) gluon bremsstrahlung.

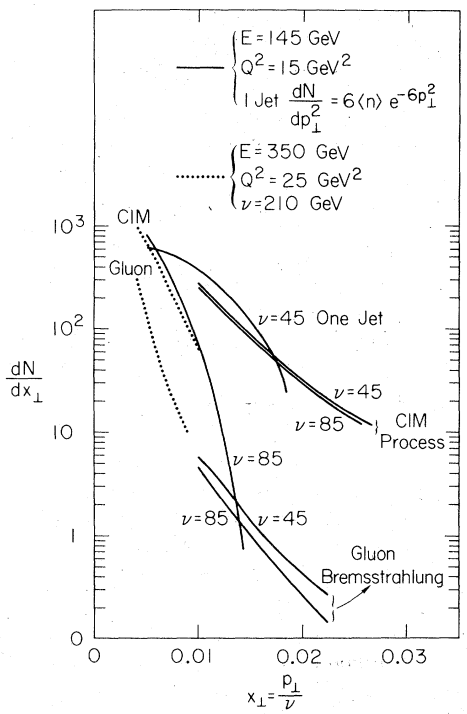

FIG. 18. The various transverse-momentum distributions in lepton-hadron deep-inelastic scattering. We have used the eikonal approximation so our results give only an order-of-magnitude estimate. The solid curves are for $Q^2 = 15$ GeV^2, $E = 145$ GeV, and $\nu = 45$ and 85 GeV. The dotted curves are for $E = 350$ GeV, $Q^2 = 25$ GeV^2, and $\nu = 210$ GeV; and $\alpha_c = 0.1$. For the single-jet process we assume $dN/dp_\perp{}^2 \propto e^{-6p_\perp{}^2}$.

from Fig. 18, we can conclude that the CIM process is the dominant contribution to the broadening of the jet structure in lepton-hadron scattering. At very large transverse momentum, it is possible that the gluonic contribution becomes the dominant effect, as suggested by the analysis of Floratos, but the cross section at such large transverse momentum falls rapidly and hence is very difficult to measure.

VII. CONCLUSION

We conclude our investigation of jet structure in e^+e^- annihilation by listing some of the more salient results which we have obtained from our calculations.

We find that jet structure in e^+e^- annihilation is very well suited to the search for gluonic structure. In comparison to hadron-hadron or lepton-hadron scattering, we feel that e^+e^- annihilation is the cleanest place to study the relation between jet structure and gluonic degrees of freedom. There are four reasons for this. First, the quarks are produced with a clean $(1+\cos^2\theta)$ angular distribution. Second, the produced quarks do not have to be folded into structure functions. Third, since there are no spectator quarks present, the rescattering problems of hadron-hadron or quark-quark interactions are minimized. Finally, the large Q^2 which can be reached in this reaction is capable of suppressing the CIM process relative to gluon emission.

One difficulty in studying jets in e^+e^- annihilation is the determination of the jet axis. This problem is due to the difficulty of detecting the neutral hadronic components of the jet. A good way to analyze the jet structure is to trigger on a leading charged hadron with $x > 0.5$, whose direction is taken to define the jet axis, and then analyze the opposite jet only.

The cleanest signal for the existence of gluons is to look at the hadronic decay of the $(J^{PC}=1^{--})$ ground state of a heavy-quark-antiquark bound system, if such a heavy quark exists. The resulting three-gluon-jet structure should be very distinct. If such a structure is present, this is a perfect place to measure the fragmentation function of a colored gluon and also an ideal place to search for quarkless states. If, on the other hand, the three-gluon-jet structure is absent (for a ground-state energy $\gtrsim$ 10 GeV), then, at the very least, our naive understanding of QCD in the asymptotically free region needs reexamination. In this respect, it would be important to calculate the hadronic decay pattern from the QCS.

We have found that jets in e^+e^- annihilation will broaden at higher energies. This broadening is due to both gluonic emission and to the emission of pions at large transverse momentum. Gluon jets can be seen only in the upper energy range of PEP and PETRA. The search for gluon jets at CESR energies will be very difficult, since the CIM process is so dominant there. In Sec. III, we have described methods to pick out the gluon bremsstrahlung process from other events. We conclude that it should probably be possible to separate gluonic-induced jet structure from competing backgrounds. In addition, if the CIM process is present there, jet structure in e^+e^- annihilation probably provides the best determination of the normalization of the quark-meson coupling of that picture. If the CIM process is absent, this would be a surprise, but not necessarily (due to our ignorance) in disagreement with QCD or the QCS.

Many explicit numerical results given in this paper assume specific forms for the gluon fragmentation function. If it should happen that the gluon fragmentation function is much more heavily suppressed everywhere, except at low x, than we have assumed, gluon fragmentation would give rise to high-multiplicity events, but events resembling three distinct jets from gluon bremsstrahlung would be suppressed. In that case, a search for high multiplicity may be more relevant. Alternatively, one can look for a broadening due to four-jet events, where each of the four jets comes from a quark fragmentation. One could study this four-jet process by detecting charged hadrons at four widely separated but fixed solid angles and search for a scaling (in Q^2) term.

Our results may be summarized most succinctly in Fig. 19, where we plot the average jet transverse momentum $\langle \bar{p}_\perp \rangle$ as a function of Q. We define

$$\langle \bar{p}_\perp \rangle = \left(\sum_i \langle p_\perp^2 \rangle_i \right)^{1/2}$$

and $\langle p_\perp^2 \rangle_i$ is the mean transverse momentum squared for the ith process

$$\langle p_\perp^2 \rangle_i = \frac{1}{\sigma_{\rm pt}} \int dp_\perp p_\perp^2 \frac{d\sigma(e^+e^- \to h_i X)}{dp_\perp} .$$

The exponential two-jet part of the cross section, $\sim \exp(-6p_\perp^2)$, yields a constant $\langle \bar{p}_\perp \rangle$ of 400 MeV/c. Including the CIM contribution raises this plateau to about 1 GeV/c. The inclusion of the gluon term leads to a $\langle \bar{p}_\perp \rangle$ which increases monotonically with Q. This occurs because of the scale invariance of gluon reactions: in particular, $\langle x_\perp \rangle$ scales, hence $\langle p_\perp \rangle$ is proportional to Q. The signal for the existence of gluon-induced jet structure is

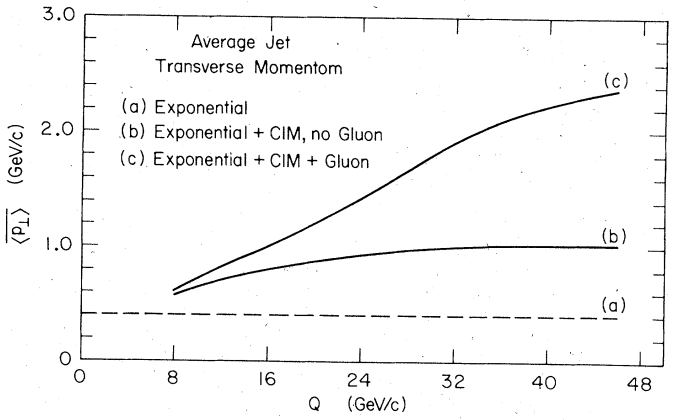

FIG. 19. Average jet transverse momentum, for the cases (a) no jet broadening, (b) jet broadening via CIM only, (c) jet broadening via CIM and gluon emission.

clearly a $\langle \bar{p}_\perp \rangle$ which increases as the center-of-mass energy increases.

It is our hope and conviction that the existence or nonexistence of gluon structure has such general consequences that its effects should be relatively insensitive to the particular assumptions we are forced to make in order to compute quantitative results. We have attempted to demonstrate that our analysis actually depends rather weakly on details, relying instead upon the asymptotic freedom of QCD and quark confinement via phenomenological fragmentation functions. We are certain that the jet structure in e^+e^- annihilation at PEP, PETRA, and CESR will help tremendously to clear up the roles QCD and the QCS play in hadron dynamics.

Of course, it will be most exciting if the transverse-momentum distribution of the jet structure at PEP, PETRA, and/or CESR energies differs from all the possibilities discussed in this work.

Note added in proof. If the recently observed Υ resonance at 9.4 GeV (Ref. 30) is really a bound state of heavy quarks, it will be an ideal place to look for the three-gluon-jet pattern discussed in Sec. V.

ACKNOWLEDGMENTS

We would like to thank our colleagues at SLAC, especially J. Bjorken, R. Blankenbecler, S. Brodsky, W. Caswell, J. Gunion, G. Hanson, R. Horgan, Minh Duong-van, J. Sapirstein, and D. Sivers for many useful discussions. We thank S. Drell and F. Gilman for valuable comments on the manuscript.

APPENDIX A: PROPERTIES OF THE QCS

Here we briefly summarize the properties of the QCS that are relevant to this work. The quark-confining string is defined by the action[6]

$$S=\int_{-\infty}^{\infty} d^2u^\alpha \sqrt{-g}\{\bar{\psi}_j[\gamma^\alpha(\tfrac{1}{2}i\overleftrightarrow{\partial}_\alpha - eB_{a\alpha}T^a)-m_j]\psi_j-\tfrac{1}{4}F^2\},$$

where $(u^\alpha,\ \alpha=0,1)$ parametrize the embedding of the string $R_\mu(u^\alpha)$, $\mu=0,1,2,3$ in four dimensions. The embedding is described locally by the tangent vector $\tau_{\alpha\mu}=\partial R_\mu/\partial u^\alpha$, the induced metric $g_{\alpha\beta}=\tau_\alpha\cdot\tau_\beta$, and $g=\det(g_{\alpha\beta})<0$. The quark fields ψ (with flavor index j) are color triplets of four-component fermions; $\{B^a_\alpha(u)\colon \alpha=0,1,\ a=1,2,\ldots,8\}$ are the two-dimensional color-SU(3) gauge fields.

The Hamiltonian can be written as

$$H=\int \mathcal{P}^{\alpha=0}_{\mu=0}\,du^1,$$

where

$$\mathcal{P}^0_\mu=\sqrt{-g}\,[\tfrac{1}{4}F^2g^{0\beta}-F^{0\sigma}F^\beta{}_\sigma+\bar{\psi}\gamma^0(\tfrac{1}{2}i\overleftrightarrow{\partial}_\beta-eB^\beta_aT^a)\psi]\tau_{\beta,\mu}$$
$$+\sqrt{-g}\,[\bar{\psi}\not{n}_l(\tfrac{1}{2}i\overleftrightarrow{\partial}^0-eB^0_aT^a)\psi]n_{l\mu}.$$

$(n_l,\ l=1,2)$ are the two spacelike normals, $n_l{}^2=-1$. Choosing the gauge $\vec{B}_1=0$, it is straightforward to show that $\vec{B}_0$ is a function of the string variables and the ψ fields. Hence the Hamiltonian can be rewritten in the following form (for color-singlet states):

$$H=\int :\psi^\dagger K\psi: du^1,$$

where K is an operator which includes the Coulomb-interaction term. We observe the following:

(1) There are no gluonic degrees of freedom.

(2) Any physical state $|p\rangle$ that has no quark modes in it will be annihilated by the Hamiltonian, $H|p\rangle=0$. In particular, the spectrum of the QCS contains no quarkless states.

(3) The ground state of the model is the vacuum. The above Hamiltonian adequately describes multihadron states. In this sense, the QCS should be considered as a field-theoretic model. (Of course, this is obvious in two-dimensional Minkowski space.)

(4) Physically, when the quark-antiquark of a meson string annihilate, a closed string can be formed. Although such a string configuration cannot survive as a physical state, it is believed to play a major role in both diffractive (as a bare Pomeron) and annihilation processes (analogous to that of a virtual photon).

The inclusion of a spin-spin term in the generalized QCS[6] does not alter any of the properties mentioned above.

APPENDIX B: DETAILS OF THE FOUR-JET CALCULATION

In this appendix we present the details of the four-jet calculation. The scattering amplitude is given by Eq. (4.2). Averaging over $e^\pm$ polarizations and summing over the final-state polarizations we find

$$\sum|T|^2=\frac{e^4g^4}{4Q^4}L^{\mu\nu}H_{\mu\nu}\ , \tag{B1}$$

where the lepton trace is

$$L^{\mu\nu}=4\{q_1,q_2\}^{\mu\nu}\equiv 4(q_1^\mu q_2^\nu+q_1^\nu q_2^\mu-q_1\cdot q_2 g^{\mu\nu})\ . \tag{B2}$$

The hadron trace $H_{\mu\nu}$ has terms proportional to q_a^2, q_b^2, and q_aq_b. It will be shown later that the q_aq_b terms do not contribute to the leading-logarithmic structure of the cross section. The q_a^2 and q_b^2 terms are related by $p_1\leftrightarrow p_3$, $p_2\leftrightarrow p_4$. Thus it suffices to consider the q_a^2 terms only. In the eikonal approximation the intermediate gluon is assumed to be relatively soft; for the q_a^2 terms that means p_2+p_3 is small compared to p_1 or p_4. The hadron trace is then vastly simplified and is given by

$$H_{\mu\nu}=128\{p_1,p_4\}_{\mu\nu}\left(\frac{p_1\cdot p_4 p_2\cdot p_3}{s_{23}^2 s_{123}s_{234}}+\frac{p_1\cdot p_3 p_1\cdot p_2}{s_{23}^2 s_{123}^2}+\frac{p_3\cdot p_4 p_2\cdot p_4}{s_{23}^2 s_{234}^2}-\frac{p_1\cdot p_3 p_2\cdot p_4+p_1\cdot p_2 p_3\cdot p_4}{s_{23}^2 s_{123}s_{234}}\right)\equiv 128\{p_1,p_4\}_{\mu\nu}K\ . \tag{B3}$$

We impose cuts on our phase-space integrations such that the final-state invariant masses s_{ijk}, s_{ij} are greater than $Q_0^2=10\ \mathrm{GeV}^2$. The jet axis is found by selecting the minimum eigenvalue of the sphericity tensor. For the fragmentation function we use Eq. (2.12). The whole computation is then done by using the numerical-integration routine of Sheppy.[28]

The leading-logarithmic structure of the total cross section can be obtained by the following analytic calculation. In addition to the approximations mentioned above we also replace the δ function in the phase space by $\delta^4(q-p_1-p_4)$ [as a check, this approximation has been applied to the three-jet case. It yields the correct $(\ln\epsilon)^2$ behavior]. Denote the polar angles of $\vec{p}_2$ and $\vec{p}_3$ relative to $\vec{p}_1$ (= $-\vec{p}_4$ in our approximation) by (θ_2,ϕ_2) and (θ_3,ϕ_3), respectively. The $\vec{p}_2$ and $\vec{p}_3$ integration we encounter is [where K is given by Eq. (B3)]

$$I=\int\frac{d^3p_2}{E_2}\frac{d^3p_3}{E_3}K$$

$$=\tfrac{1}{8}\int dE_2dE_3d\cos\theta_2d\cos\theta_3d\phi_2d\phi_3(I_1+I_2)\ , \tag{B4}$$

where

$$I_1=\{[E_2(1-\cos\theta_2)+E_3(1-\cos\theta_3)]\times[E_2(1+\cos\theta_2)+E_3(1+\cos\theta_3)]\times[1-\cos\theta_2\cos\theta_3-\sin\theta_2\sin\theta_3\cos(\phi_2-\phi_3)]\}^{-1}$$

and

$$I_2=-2E_2E_3(\cos\theta_2-\cos\theta_3)^2I_1^2\ . \tag{B5}$$

The integration over ϕ_2 and ϕ_3 can be easily performed. Making the following change of variables

$$w=\frac{E_2}{Q}(1-\cos\theta_2),\quad x=\frac{E_3}{Q}(1-\cos\theta_3),$$
$$y=\frac{E_2}{Q}(1+\cos\theta_2),\quad z=\frac{E_3}{Q}(1+\cos\theta_3), \tag{B6}$$

we find

$$I=\frac{\pi^2}{4}\int\frac{dw\,dx\,dy\,dz}{|wz-xy|}\frac{wy+xz}{(w+x)^2(y+z)^2}\ . \tag{B7}$$

The lower limits of integration are given by $s_{ijk}\geq Q_0^2=Q^2\epsilon$. Translating into the lower limits of s_{ij} this cut in the phase-space integrations means w, x, y, z, s_{14}/Q^2, and s_{23}/Q^2 are all greater than $\epsilon/3$. The last condition (in the azimuthally averaged sense) implies $|wz-xy|>\epsilon/3$. The upper limits of integration can be easily seen to be restricted by $x+y+w+z+|wz-xy|+\epsilon/3=1$. For the most divergent logarithmic structure the integrations yield

$$I=\tfrac{2}{3}\pi^2|\ln\epsilon|^3\ . \tag{B8}$$

Performing the trivial $\vec{p}_1$ and $\vec{p}_4$ integrations

$$\int\frac{d^3p_1}{E_1}\frac{d^3p_4}{E_4}\delta^4(q-p_1-p_4)\{q_1,q_2\}^{\mu\nu}\{p_1,p_4\}_{\mu\nu}=\tfrac{32}{3}\pi E^4\ , \tag{B9}$$

summing over the colors of the final-state particles

$$\sum_{i,j}\mathrm{Tr}\left(\frac{\lambda^i}{2}\frac{\lambda^j}{2}\right)\mathrm{Tr}\left(\frac{\lambda^i}{2}\frac{\lambda^j}{2}\right)=2\ , \tag{B10}$$

and putting all the factors together, we get

$$\sigma=\frac{32}{9\pi}\frac{\alpha^2\alpha_c^2}{Q^2}|\ln\epsilon|^3\sum_{a\neq b}(q_a^2+q_b^2)$$
$$=\frac{32}{9\pi}\frac{\alpha^2\alpha_c^2}{Q^2}|\ln\epsilon|^3(N-1)\sum_{\text{flavors}}q_a^2\ , \tag{B11}$$

where N = number of quark flavors.

Finally we have to show that the q_aq_b terms do not contribute to order $|\ln\epsilon|^3$. The hadron trace involved is

$$H_{\mu\nu}=-2q_aq_b[f_{\mu\nu}(1,4,2,3)+f_{\mu\nu}(4,1,3,2)-f_{\mu\nu}(1,4,3,2)-f_{\mu\nu}(4,1,2,3)]\ , \tag{B12}$$

where

$$f_{\mu\nu}(1,4,2,3)=\frac{1}{s_{14}s_{23}s_{134}s_{234}} \times \mathrm{Tr}(\not p_1\gamma^\alpha \not p_4\gamma^\beta \not p_{234}\gamma_\mu) \times \mathrm{Tr}(\not p_2\gamma_\beta \not p_3\gamma_\alpha \not p_{134}\gamma_\nu). \quad \text{(B13)}$$

The product of the traces can be done by the algebraic manipulation routine REDUCE.[29] Notice that the denominators in the $f_{\mu\nu}$'s are less singular than those in the $(q_a^2+q_b^2)$ terms. By explicit calculation we have found that the q_aq_b terms can at most contribute to order $(\ln\epsilon)^2$.

*Work supported by the U.S. Department of Energy.

[1]G. Hanson *et al.*, Phys. Rev. Lett. 35, 1609 (1975); G. Hanson, in *Proceedings of the XVIII International Conference on High Energy Physics, Tbilisi, 1976,* edited by N. N. Bogolubov *et al.* (JINR, Dubna, U.S.S.R., 1977), Vol. II, p. B1.

[2]J. D. Bjorken and E. A. Paschos, Phys. Rev. 185, 1975 (1969); S. D. Drell, D. J. Levy, and T.-M. Yan, Phys. Rev. D 1, 1617 (1970); see also R. P. Feynman, *Photon-Hadron Interactions* (Benjamin, Reading, Mass., 1972).

[3]O. W. Greenberg, Phys. Rev. Lett. 13, 598 (1964); H. Fritzsch, M. Gell-Mann, and H. Leutwyler, Phys. Lett. 47B, 365 (1973); W. Bardeen, H. Fritzsch, and M. Gell-Mann, in *Scale and Conformal Symmetry in Hadron Physics,* edited by R. Gatto (Wiley, New York, 1973), p. 139.

[4]H. D. Politzer, Phys. Rev. Lett. 30, 1346 (1973); D. Gross and F. Wilczek, *ibid.* 30, 1343 (1973); G. 't Hooft, Nucl. Phys. B61, 455 (1973).

[5]See, e.g., K. Wilson, Phys. Rev. D 10, 2445 (1974); J. Kogut and L. Susskind, Phys. Rev. D 11, 395 (1975); W. A. Bardeen and R. Pearson, Phys. Rev. D 14, 547 (1976).

[6]S.-H. H. Tye, Phys. Rev. D 13, 3416 (1976); Y. J. Ng and S.-H. H. Tye, *ibid.* 16, 2468 (1977).

[7]Here we can include the MIT bag model as a modified version of QCD; see A. Chodos, R. L. Jaffe, K. Johnson, C. B. Thorn, and V. F. Weisskopf, Phys. Rev. D 9, 3471 (1974); and for its phenomenology, T. DeGrand, R. Jaffe, K. Johnson, and J. Kiskis, Phys Rev. D 12, 2060 (1975).

[8]Cf. D. Gross and F. Wilczek, Phys. Rev. D 8, 3633 (1973); H. Georgi and H. D. Politzer, Phys. Rev. D 9, 416 (1974); Harvard report, 1976 (unpublished).

[9]R. C. Giles and S.-H. H. Tye, Phys. Rev. Lett. 37, 1175 (1976); Phys. Rev. D 16, 1079 (1977).

[10]For an explanation of scaling violation in the parton model, see, e.g., I. Schmidt and R. Blankenbecler, Phys. Rev. D 16, 1318 (1977).

[11]We have not included in our consideration the recent exciting development of the pseudoparticle solution in QCD in relation to the U(1) problem. [See A. Belavin, A. Polyakov, A. Schwartz, and Yu. Tyupkin, Phys. Lett. 59B, 85 (1975); G. 't Hooft, Phys. Rev. Lett. 37, 8 (1976).] A comparison of these solutions with experiment is not possible at this moment.

[12]For estimates of the masses of pure gluon states, cf. P. G. O. Freund and Y. Nambu, Phys. Rev. Lett. 34, 1645 (1975); J. Willemsen, Phys. Rev. D 13, 1327 (1976); R. Jaffe and K. Johnson, Phys. Lett. B60, 201 (1976).

[13]For a review, cf. J. D. Bjorken, in *Proceedings of Summer Institute on Particle Physics, 1975,* edited by M. Zipf (SLAC, Stanford, California, 1975), p. 85.

[14]D. E. Soper, Phys. Rev. Lett. 38, 461 (1977); R. F. Cahalan, K. Geer, J. Kogut, and L. Susskind, Phys. Rev. D 11, 1199 (1975); R. Cutler and D. Sivers, *ibid.* 16, 679 (1977); S. J. Brodsky, W. Caswell, and R. Horgan (unpublished).

[15]E. G. Floratos, CERN Report No. TH-1992, 1977 (unpublished).

[16]J. Ellis, M. K. Gaillard, and G. Ross, Nucl. Phys. B111, 253 (1976). We refer to this work in the text as EGR.

[17]See, e.g., *Dual Theory,* edited by Maurice Jacob (North-Holland, New York, 1974).

[18]G. 't Hooft, Nucl. Phys. B75, 461 (1974); C. G. Callan, N. Coote, and D. J. Gross, Phys. Rev. D 13, 1649 (1976); M. B. Einhorn, Phys. Rev. D 14, 3451 (1976).

[19]R. Blankenbecler, S. J. Brodsky, and J. F. Gunion, Phys. Lett. 39B, 649 (1972); Phys. Rev. D 6, 2652 (1972); Phys. Lett. 42B, 461 (1973). S. J. Brodsky and G. Farrar, Phys. Rev. Lett. 31, 1153 (1973); Phys. Rev. D 11, 1309 (1975). For a review, see D. Sivers, R. Blankenbecler, and S. J. Brodsky, Phys. Rep. 23C, 1 (1976).

[20]S. J. Brodsky and J. Gunion, Phys. Rev. Lett. 37, 402 (1976).

[21]J. D. Bjorken and S. J. Brodsky, Phys. Rev. D 1, 1416 (1970).

[22]We follow C. T. Sachrajda, and R. Blankenbecler, Phys. Rev. D 12, 3624 (1975).

[23]S. J. Brodsky, R. Blankenbecler, and J. Gunion (unpublished); our $(g/4\pi)$ is their g. See also M. Duong-van, K. V. Vasavada, and R. Blankenbecler, Phys. Rev. D 16, 1389 (1977).

[24]There are numerous conjectures on the existence of heavy quarks. See, e.g., R. M. Barnett, Phys. Rev. Lett. 36, 1163 (1976); F. Gürsey and P. Sikivie, Phys. Rev. Lett. 36, 775 (1975); B. W. Lee and S. Weinberg, Phys. Rev. Lett. 38, 1237 (1977).

[25]F. J. Gilman, in *Proceedings of the 1975 International Symposium on Lepton and Photon Interactions at High Energies, Stanford, California,* edited by W. Kirk (SLAC, Stanford, 1976). See also Ref. 13.

[26]S. M. Berman, J. D. Bjorken, and J. B. Kogut, Phys. Rev. D 4, 3388 (1971).

[27]We use

$$\nu W_2(x) = F(x) = \begin{cases} 90\,x^{3/2}e^{-7.5x} & \text{for } x<0.35 \\ 5(1-x)^3 & \text{for } x>0.35. \end{cases}$$

[28]This program is described by A. J. Dufner, in Proceedings of the Colloquium on Computational Methods in Theoretical Physics, Marseille, 1970 (unpublished).

[29]A. C. Hearn, Stanford University Report No. ITP-247 (unpublished).

[30]S. W. Herb *et al.*, Phys. Rev. Lett. 39, 252 (1977).